DESIGN OF AN ADVANCED COMPOSITE SHELL FOR HELICOPTER PILOT HELMETS

A THESIS SUBMITTED TO
THE GRADUATE SCHOOL OF NATURAL AND APPLIED SCIENCES
OF
MIDDLE EAST TECHNICAL UNIVERSITY

BY

EZGİ SÜNEL

IN PARTIAL FULFILLMENT OF THE REQUIREMENTS
FOR
THE DEGREE OF MASTER OF SCIENCE
IN
MECHANICAL ENGINEERING

FEBRUARY 2012

Approval of the thesis:

DESIGN OF AN ADVANCED COMPOSITE SHELL FOR HELICOPTER PILOT HELMETS

submitted by **EZGİ SÜNEL** in partial fulfillment of the requirements for the degree of **Master of Science in Mechanical Engineering Department, Middle East Technical University** by,

Prof. Dr. Canan Özgen _____
Dean, Graduate School of **Natural and Applied Sciences**

Prof. Dr. Suha Oral _____
Head of the Department, **Mechanical Engineering**

Prof. Dr. Levend Parnas _____
Supervisor, **Mechanical Engineering Dept., METU**

Examining Committee Members:

Prof. Dr. Levend Parnas _____
Mechanical Engineering Dept., METU

Prof. Dr. Can Çoğun _____
Mechanical Engineering Dept., METU

Prof. Dr. Suat Kadıoğlu _____
Mechanical Engineering Dept., METU

Asst. Prof. Dr. Merve Erdal _____
Mechanical Engineering Dept., METU

Dr. Devrim Anıl _____
Mechanical and Optical Design Dept.,
Aselsan Inc.

Date: 01.02.2012

I hereby declare that all information in this document has been obtained and presented in accordance with academic rules and ethical conduct. I also declare that, as required by these rules and conduct, I have fully cited and referenced all material and results that are not original to this work.

Name, Last Name: Ezgi SÜNEL

Signature:

ABSTRACT

DESIGN OF AN ADVANCED COMPOSITE SHELL FOR HELICOPTER PILOT HELMETS

Sünel, Ezgi

Ms., Department of Mechanical Engineering

Supervisor: Prof. Dr. Levend Parnas

Fabruary 2012, 94 pages

This thesis reports on a design study, conducted for an advanced composite helmet shell for helicopter pilots. The helmet shell is expected to provide a level of protection against low velocity impacts with its weight criteria. Therefore, ergonomy, light weight, and the ability to withstand low velocity impact became the main issues for this study. For this purpose, an experimental program has been developed including low velocity impact tests on specimens. The drop height, drop weight, specimen stacking sequences and size were constant parameters. Test specimens were produced using the plate size of 220x220 mm having different thicknesses. Specimen materials were aramid, carbon, and a hybrid form of these two. Thus, the parameters of the study were specimen thickness and the material types.

The impact tests are carried out on a specially designed test rig. The design decisions are made in accordance with the results of the experiments. In compliance with the lightweight and manufacturing criteria, the hybrid specimen was selected helmet shell.

For the purpose of ergonomy a geometric design was also conducted from

headfrom sizes of Turkish Army by using 3D design software. After specifying the composite material, manufactured helmet shell was tested in another test rig according to the ANSI Z90.1.1992. For the requirement of the acceleration level 300g, the helmet shell design was found to be successful at seven different and critical impact points.

Keywords: Helicopter helmet, low velocity impact, carbon, aramid, epoxy, laminated composite, hybrid composite

ÖZ

HELİKOPTER PİLOTLARI İÇİN İLERİ KOMPOZİT KASK KABUĞU TASARIMI

Sünel, Ezgi
Yüksek Lisans, Makina Mühendisliği Bölümü
Tez Yöneticisi: Prof. Dr. Levend Parnas
Şubat 2012, 94 sayfa

Bu tezde, helikopter pilotlarının kullanacağı ileri teknoloji kompozit kask tasarım çalışması yürütülmüştür.Kaskın düşük hızlı darbelere karşı belli bir dayanım göstermesi beklenmekle birlikte ağırlık kriteri de önem teşkil etmektedir. Bu nedenle bu çalışmada, ergonomik tasarım, hafiflik ve düşük hızlı darbelere dayanım temel kriterler olmuştur. Bu amaçla, değişik malzeme kombinasyonları üzerindeki düşük hızlı darbe testlerini içeren deneysel bir çalışma yürütülmüştür. Düşü yüksekliği, düşü ağırlığı, numune katmanların sıralanışı ve numune boyutları sabit tutulmuştur. Değişik kalınlıklara sahip 220x220 mm boyutlarında plakalar üretilmiştir. Numunelerde kullanılan malzemeler, aramid ve karbon takviyeli epoksi ile bunların kombinasyonlarından oluşmaktadır. Böylece, numune kalınlığı ve malzeme çeşidi bu çalışmanın değişken parametreleri olarak ele alınmıştır.

Darbe deneyleri sadece bu deney için tamamen yenilenen bir deney düzeneğinde yapılmıştır. Deney sonuçlarıyla birlikte hafiflik ve üretim kriterleri de düşünüldüğünde hibrid numune en uygun malzeme olarak seçilmiştir.

Ergonomi çalışması için Silahlı kuvvetlerdeki askeri personelin kafa ölçüleri temel alınarak geometrik tasarım çalışması yürütülmüştür. Deneylerle belirlenen malzeme ve tasarlanan geometriye sahip kaskın üretimi yapılmıştır. ANSI Z90.1.1992

standardına göre kask için tasarlanmış deney düzeneğinde üretilen kaskın testleri yapılmıştır. Standartta belirtilen yedi darbe noktasındaki 300 g ivme seviyesi sağlanmış olup, kask ANSI standardına uygun olarak yapılan testten geçmiştir.

Anahtar Kelimeler: Helikopter kaskı, düşük hızlı darbe, karbon, aramid, epoksi, katmanlı kompozit, hibrid yapılı kompozit

To My Family

ACKNOWLEDGEMENTS

The author wishes to express her sincere appreciation to her thesis supervisor Prof. Dr. Levend Parnas for his guidance, advice, encouragements and helpful criticism throughout the research.

The author would like to thank ASELSAN, Inc. and her project manager at ASELSAN, Miss. Seçkin Tunalılar, for her support for manufacturing the "Tools for Impact Test Setup". The author also want to thank to Mr. Tolga Ziya Sander for his valuable and beneficial support and advices in her study.

Also, the author wishes to express her sincere appreciation to technical assistance of Assoc. Prof. Dr. Özgür Anıl, and his precious help for the use of "Impact Test Setup" at Gazi University Civil Engineering Laboratory. Moreover, the author would like to thank Barış Elektrik Inc. and CES Inc. for their support of producing this study's composite specimens.

Moreover very preciously, the author would like to thank to Dr. Devrim Anıl for his support, technical assistance and his supervision in every step of her study. And also the deepest gratitude goes to Pınar De Neve for her support to this thesis and in my life since the high school.

Last, but certainly not least, the author wishes to offer her thanks to her parents for their continuous help and understanding during the thesis study.

TABLE OF CONTENTS

LIST OF TABLES

LIST OF FIGURES

LIST OF SYMBOLS

ANSI:	American national standards institute
APW:	Aramid plain weave
ASTM:	American society for testing and materials
CFRP:	Carbon fiber reinforced plastics
CTW:	Carbon twill weave
GL:	Glass fabrics
GR:	Graphite fabrics
GTW:	Glass twill weave
ICP:	Integrated circuit piezoelectric
MAT:	Material model
TGS:	Trial glass specimen
TCS:	Trial carbon specimen
USAARL:	Unites States Army Aeromedical Research Laboratory
v_f :	Volume fraction of fibers
W_f :	Weight of fibers
ρ_f :	Density of fibers
W_c :	Weight of composite
ρ_c :	Density of composite

CHAPTER 1

INTRODUCTION

1.1 Motivation

Helmets are used to protect the wearer's head from damage caused by a variety of external impacts They are used in various environments such as vehicles and aircraft and in many sports for example; American football, cricket and rock climbing. The types of helmets and materials used in manufacturing vary depending on the use of helmets.

There are several important issues to be considered when designing a helmet. The helmet should be light and has to protect the wearer's head from various external impacts. The disciplines of human engineering, mechanical engineering and material science engineering are combined in order to design helmets with high protection levels and maximum ergonomy.

The design of the shell of the helicopter pilot helmet's was by motorcycle helmet designs. There are many designs of helmets for commercial helicopter pilots manufactured all over the world some of these are shown in Figure 1.1 to Figure 1.3. According to the potential use the shape and weight of the helmets differ. The main sub components of the helmet; the retention system, liner, earcups and the visor also the shape and weight of the helmets. The shell is the main part of a helicopter helmet and its main function is to protect the user. The retention system holds the subparts of the helmet together. The liner consisting of a foam material and the shell combine to absorb the impact energy. Although the liner absorbs more

impact energy, the shell is directly exposed to the impact. The earcups are vital parts of the audio communication system in the helicopter. Lastly, the visor is used as a screen to display information from control system and important data from the flight instruments. These subcomponents are described later in 3D design section in Chapter 5 .

Figure 1.1 Alpha Eagle® Helicopter Helmet [21]

Figure 1.2 Gentex® HGU 56 Helicopter Helmets [36]

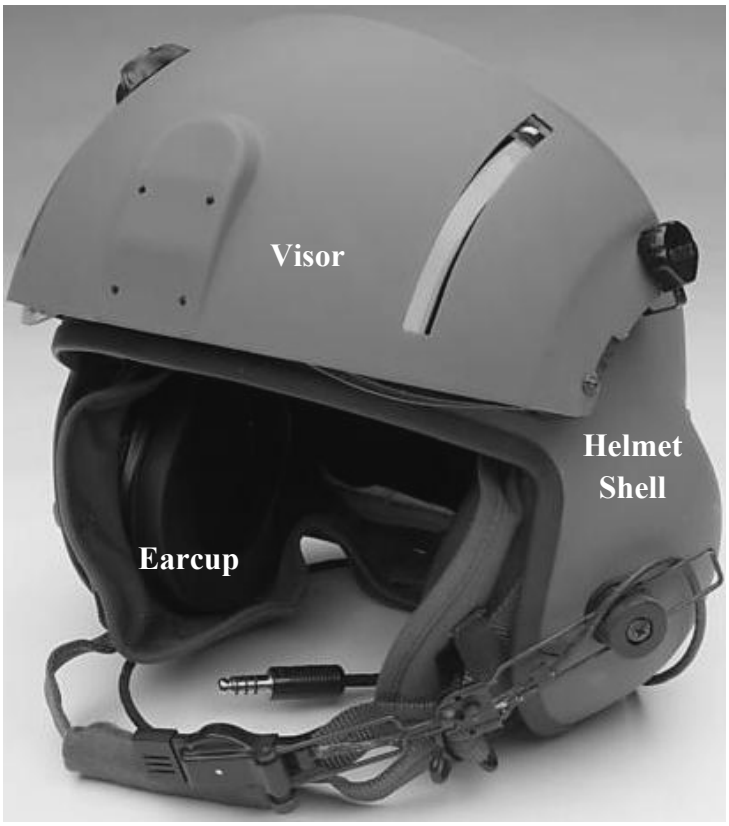

Figure 1.3 Gentex® SPH 4B Helicopter Helmet [37]

The design of the helmet, shell thickness, material type and composition of composite material should be determined based on experimental data which includes, impact tests, penetration tests and retention system strength tests performed according to the ANSI.Z90.1 1992 standard. According to this standard, a helicopter pilot helmet should withstand impacts up to 300g, however, these helmets are not generally required to have ballistic protection.

The market for helicopter helmets is for military use, examples of various helmet types and technical specifications used in the U.S. army until 1995 are shown in Table 1.1. Because of the knowhow criteria after 1995 there is limited knowledge about helmet specifications.

Table 1.1 Chronology of U.S Army Aviation Helmets and Their Characteristics [29]

Year	Helmet	Characteristic
1960	APH-5	Navy design, general purpose
1969	SPH-4	New shell contour, improved sound attenuation, general purpose
1974	SPH-4	35% thicker foam liner
1982	SPH-4	Thinner shell
1984	IHADSS	Equivalent to SPH-4, specific to AH-64 aircraft
1989	SPH-4B	New shell material, liner, fitting, retention, earcups, and visor systems(lower weight)
1995	HGU-56P	All new, general purpose and aircraft unique design (improved impact protection)

1.2 Composite Material Selection for the Shell of a Helicopter Pilot Helmet

The detail of the design of these composite helmets is mostly confidential and covered by highly classified patents and thus, there is not much academic research on this topic. Thus we can conclude, the design of a composite helicopter helmet is a “know how” technology.

The ANSI Z90.1 [32] standard defines a low velocity impact criterion for vehicular helmets, including composite helicopter helmets. Therefore, the designer should choose impact protected fibers, matrix, orientation and thickness to conform to this criterion.

Glass fiber reinforcement thermosetting plastic (GFRP) is widely used in safety helmets however, it is relatively heavy and there are certain limitations to the production of a large size helmet therefore , other reinforcement materials should

be considered. Aramid and carbon reinforcement materials can be used to produce an impact resistant and light weight helmet. Aramid has high tenacity and high modulus and carbon has a good strength and mechanical behavior. Hence, a hybrid structure can be more effective for the manufacture of helmets. Moreover, literature shows that the aramid/epoxy composites are generally used for helmets requiring impact and ballistic protection. Since there is limited information concerning the stacking sequence of the composite materials to be used in the helmet, therefore, it is necessary to carry out experiments using a constant stacking sequence in order to accurately interpret the experiment results.

1.3 Aim and Scope of this Thesis

The use of composite materials in helmet design is very important for military applications. Over the years numerous studies have been undertaken to find the optimum materials to satisfy the requirements for a helmet shell that has impact energy absorption and is light weight.

This study focuses on both finding a light composite material for a helicopter pilot helmet shell and satisfying the impact requirements. The experiments were performed to investigate the effects of defined parameters on structural design of a composite material. In this study, the specimen thickness and composite material types, especially fiber types, were considered as variable parameters based on the light weight criteria and impact resistance. The fixed parameters were; the impact drop weight, impact drop height, stacking sequence and specimen size.

A literature survey was also carried out to find the optimum composite material. As a result, carbon fibers and aramid were selected for the test specimens with similar orientations but different thicknesses. The damage to carbon reinforcement upon impact has been comprehensively studied but there is less information about the aramid reinforcement impact phenomenon and a lack of through investigation about

certain hybrid composites in the literature. Thus, this study contributes to the literature concerning the effects of parameters on the selection of an optimum material for helmet shells. For this purpose 6 type of composite specimens were manufactured to test their low velocity impact ability in the light of ANSI Z90.1 1992 standard.

Prior to the experiments being carried out, a drop weight impact test rig was designed to test the larger specimens in Gazi University. Furthermore, since the previous test rig's ability was not capable of accurately capturing the required acceleration and force levels, a new specimen holder housing was designed and the appropriate test rig components for smaller size test specimens were added such as a load cell and accelerometers. Furthermore, by using the acceleration and force data, it was possible to determine the velocity and displacement history of the drop weight and the corresponding absorbed impact energy.

While determining the appropriate composite material, a parallel study for the 3D helmet shell design was conducted. The inner shape of the helmet is very important for the user; it must be comfortable, easy to wear and remove. Thus, the pilot's head geometry should be taken into account in the 3D design of helmet. The results from the literature review of the anthropometric data was useful in designing the optimum form of the helmet. The headform was designed according to the specifications in Donelson's work [30] and measurements from the study by Kayış [31]. Furthermore, the form of the helmet shell is affected from the subcomponents of the helmet system. The liner, retention system, visor and earcups play an important role in the final shape of the helmet shell. Liner is a foam material which mainly protects the head from impact. The retention system is also an inner element of the helmet system that places the helmet to the head like a hairband in a comfortable way. Visor is a kind of display module that is aligned with the eyes of the pilot and positioned in front of the helmet system. Finally, earcups as the other inner element are used for sound communication.

The helmet shell design manufactured with the hybrid material selected following

the specimen tests, was tested according to the low velocity impact criteria. The impact test of the helmet shell was carried out by Barış Elektrik Inc. and the details of the test rig and the related experiments are given in Chapter 6

CHAPTER 2

LITERATURE SURVEY

2.1 Introduction

The literature review was undertaken concerning two important issues concerning helmet shell design. These were the behavior of various composite materials under low velocity impact and the related test setups for measuring the impact resistance of the composite plates. Low velocity test setups, their experiment devices, composite material types, tried thicknesses of the test specimens and their layer configuration constituted the parameters of the literature review.

Although not considered a hard and fast rule, the impact phenomenon has been classified, based on the impactor velocity, into low (< 250 m/s), medium (250-2000 m/s), ballistic (2000-12000 m/s) and hyper velocity (>12000 m/s) impacts [5]. The behavior of the composite structures under low velocity impact has been studied by many researchers, including experimental, numerical and analytical works. However, most of the publications report on low velocity impact experiments using flat plates [1- 18].

Early impact test methodologies have already been developed for the investigation of metal specimens using the techniques of the Izod, Charpy and Hounsfield tests. In the 1970s these tests were conducted on composite materials in order to determine the mechanical properties of composite materials [26]. Table 2.1 summarizes the development of the early impact tests from 1970 to 1973.

Table 2.1 Traditional Early Impact Tests [11]

Year	Author	Test	Test Details
1970	Hazell	Hounsfield Tensometer	Strain rate experiment
1971	Hazell	Izod Impact Pendulum	Obtained data for speeds from 0,. to 3.5 m/s.
1971	Hancox	Izod Impact Test	Studied carbon fiber reinforced plastics and found that impact energy increased with increasing fiber volume fraction.
1971	Hancox and Wells	Three Point Loading Test	Showed that the flexural strength and stiffness of glass-fiber composite beams can be increased applying a carbon-fiber layer to the top and bottom of the composite (hybrid structure).
1973	Hancox and Wells	Izod Impact Test	Measured the impact strength, flexural modulus and flexural strength, although their improvement on test specimen dimensions, all specimens failed under impact conditions.
1975	Harris and Bunsell	Charpy Impact Test	Tested the tensile strength of hybrid carbon and glass fiber composites, also used the Hancox and Wells Charpy impact test forhybrid composites. They found that for notch specimens the impact energy varied according to the proportions of glass reinforced plastic (GRP) and CFRP, and also that the flexural modulus varied linearly with the volume fraction.

Table 2.1 Traditional Early Impact Tests [11] Cont'd.

Year	Author	Test	Test Details
1975	Perry and Adams	Charpy Impact Test	Investigated the impact response of graphite epoxy hybrid composites. The result was that the material and the layup was a significant factor in the impact energy absorption.

Although these early impact test methodologies are useful in gaining an understanding of some of the properties of composites, it is not possible to validate the experimental results due to the test specimen geometries used in these tests. Some researchers based their impact experiments on traditional methods related to metal testing. Instead of these methods, they used gas gun tests with high velocity and low velocity drop-weight impact rigs which provide more accurate results compared with early impact tests. Table 2.2 summarizes the early test methods used on composite impact properties and their development.

Table 2.2 Early Impact Tests[11]

YEAR	AUTHOR	TEST	TEST DETAILS
1971	Rogers et al.,	Air gun	High speed ballistic impact tests on square composite laminates, to evaluate impact resistance. The authors proved that the air gun test was more suitable for small particle impacts on composite materials.
1972	Wrzesien	Air gun	Used wire sheet reinforcements for fiber glass composites to improve the resistance of composites to high velocity impact. The results of this study provided an improvement to both impact resistance and the damage arc on the composite.
1973	Thomas	Non-instrumented drop weighting rig	Evaluated environmental effects on the impact strength of fiber glass polyester. The result was that the performance of composite could be reduced by a scratch or a notch on the surface of the composite.

From a literature review, Sevkat et. al [14] summarized the parameters which affect the impact performances of the composites as: the shape of the impactor, impact velocity, weaving angles between interlacing yarns, stitching, and water immersion aging on the drop-weight impact responses.

Abrate et. al [24] review the literature up to 1994 concerning the impact on laminated composites. His focus was threefold; first, to understand the dynamics of the impact on a composite structure by an object, and the measurement of the contact force history and the total response of the body. Second, understanding how

impact damage develops, the type of failure modes that occur and the factors affect damage resistance. Lastly, the estimation of affect of the impact damage on he mechanical properties of the structure.

Padaki et al. [5] defined the parameters for impact instrumentation as; drop height (velocity), drop mass, angle of impact and impactor details such as type, size and geometry,. They stated that the thickness, fiber volume fraction (V_f), stacking sequence, elastic properties and resin system utilized all played important roles in the impact behavior of a composite material.

Some authors have worked on specific composites to understand the effects of drop weight low velocity impact and others have chosen hybrids. Furthermore, different test rigs were used and the experiments were carried out in different sequences. In more recent times more research has been undertaken with different experimental setups to investigate low velocity impact as detailed in the section below

2.2 Survey on Low Velocity Impact Experiment Test Setups

Belingardi and Vadori et. al [17] worked on composite material plates to investigate the impact phenomena using dart test setup according to the ASTM D3029 standard This test setup includes a free fall drop dart machine with no energy storage device and a fixed mass impactor. This standard equipment is used to acquire, sample, collect and store the signal from a load cell positioned near the head of the falling dart. The Instron®-Dynatup® 9250 HV model tester was used by Sayer et. al [1]. This test setup consists of a dropping crosshead with its accessories, a pneumatic clamping fixture, a pneumatic rebound brake, and Dynatup® 930-I impulse data acquisition system. Dahsin et. al [25] used Dynatup® GRC 8200 for impact testing (Figure 2.1). This test setup includes an impactor consisting of a dropping crosshead, an impactor rod, and an impactor nose. Aslan et. al [15] designed a low velocity impact vertical drop-weight test setup (Figure 2.2). To measure the impact force history, a Brüel and Kjaer 8201 type piezoelectric force transducer is mounted to the bottom side of a steel cross-bar. She used NEXUS®-2692 A OI1 to amplify

signals from a piezo electric force transducer. Sevkat et. al [14] used a pressure assisted Instron®-Dynatup® 8520 tester, a steel mass impactor, a pneumatic clamp and strain gauges for drop weight impact testing for four different energy levels. From the above test setups in literature, the main parts of the used setup was designed. All the rigs for an impact drop weight test detailed above consisted of the impactor, a clamping fixture, piezo electric sensors and a data acquisition system . These items were selected according to the measurements to be obtained from the composite test specimens. Acceleration, force and absorbed impact energies were common phenomenon from the test setups of literature survey.

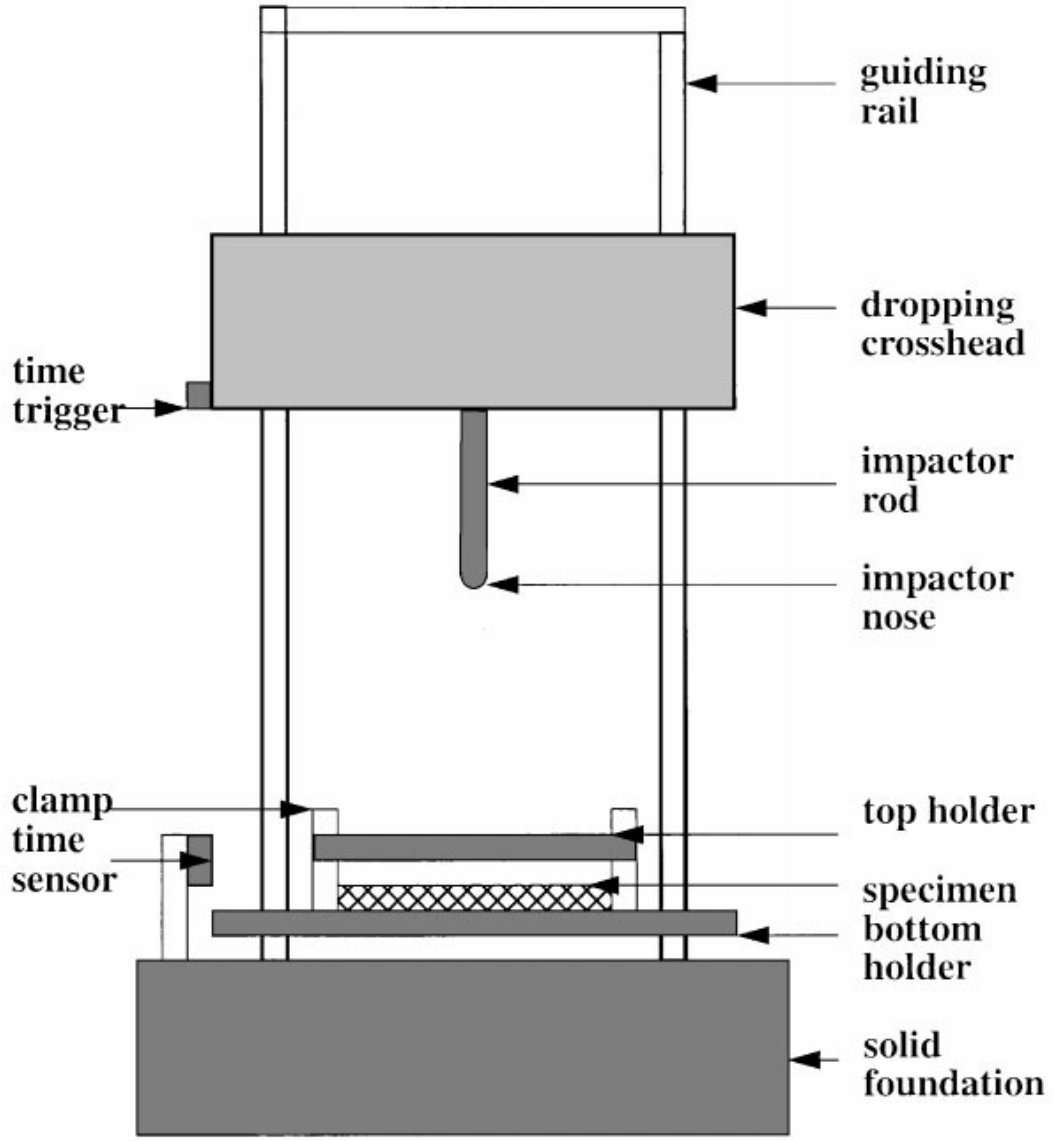

Figure 2.1 Example Schematic Diagram of an Impact Test Machine [25]

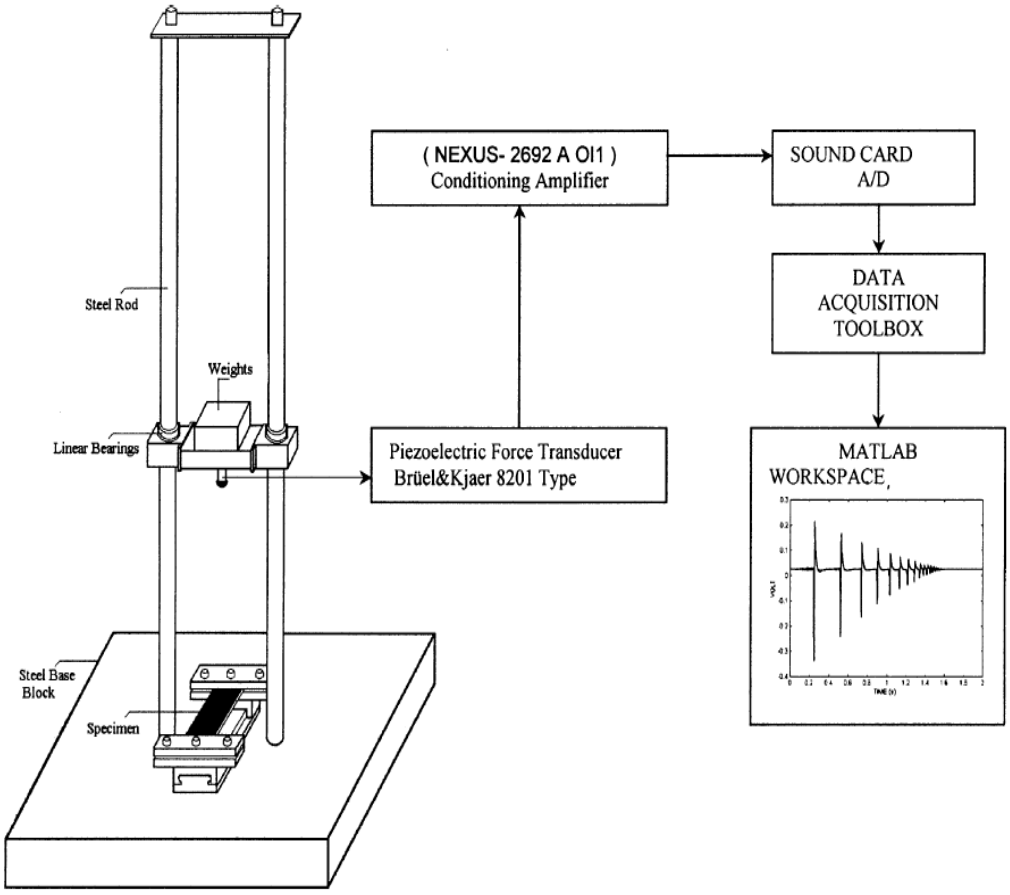

Figure 2.2 R_z Example Schematic Diagram of an Impact Testing Apparatus [15]

2.3 Fiber Glass Composite Plates under Low Velocity Impact

Naik et al., [6] carried out research on fiber glass woven fabric laminated composite plates (Figure 2.3) under transverse central low velocity point impact. They assessed the impact using a finite element formulation and the behavior of the composites was evaluated using the Tsai Hill quadratic failure criterion. Naik et al., compared the impact behavior of balanced, symmetric and cross-ply unidirectional laminates with the woven fabrics. In these numerical experiments they used 150 mm x 150mm x 6mm square plates with a steel spherical impactor, which had 6.5 mm radius, modulus elasticity of 200 GPa and Poisson's ratio of 0.3. The density of

E-glass fiber was 2620 kg/m^3 and for epoxy resin it was 1170 kg/m^3. The experimental laminates stacking sequences were for the cases of $[0/90]_s$ and $[0]_n$. Naik et al., tested the impacted specimens with initial velocities of 3 m/s and 1 m/s with the boundary conditions of a simply supported beam.

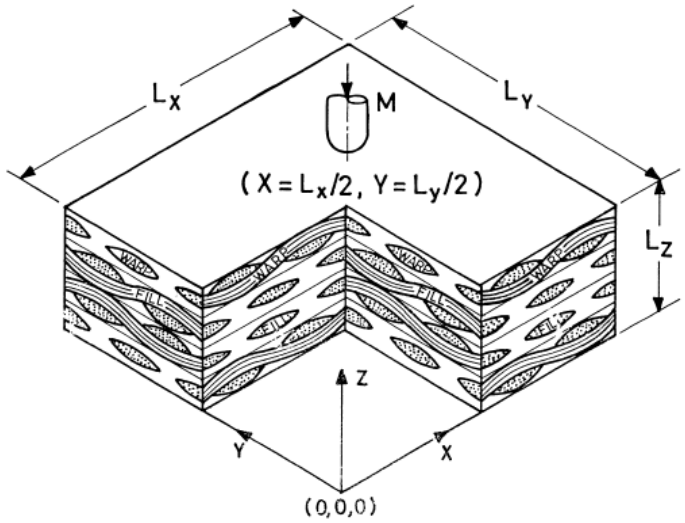

Figure 2.3 Schematic of a woven fabric plate [6]

Belingardi et al., [7] carried out experiments on fiber glass epoxy laminates for both unidirectional and woven layers with three different layer orientations of $[0/90]_s$, $[0/60/-60]_s$ and $[0/45/-45]_s$. The dimensions of the six different types of plates were 100mm x 100 mm x 2mm and the fiber reinforcement was 62-66 % which was constant for each plate. Furthermore, the density of the plates was 1.99 kg/dm^3. They aimed to describe the impact behavior of the material using the following energy absorption parameters; saturation impact energy and damage degree of the composite, values of impact force history (first damage force and the maximum force) and the sensitivity of the materials mechanical characteristic to the strain rate effect. The test setup was a free fall drop dart machine with no energy storage device. The maximum impact energy was limited by adjustable height with a maximum of about 2000 mm. Thus, the peak energy was approximately 400J with an impact velocity 6.28 m/s supplied by gravity.

Aslan et al., [15] study is about evaluation of in-plane dimensional effect of fiber glass reinforced epoxy laminated composites under low velocity impact. They used in the tests an impactor which is 18 mm in diameter. The maximum height of the impactor is 1032 mm which provides 4.5 m/s initial velocity. The tests are done with a constant velocity 3 m/s with the varied mass for two cases 135 and 2600g. The stacking sequence of laminated composite was $[0/90/0/90]_s$ oriented cross ply E-glass/epoxy and a volume fraction 57% in fibers with different plate dimension as: 150mm x 150mm x 4.8 mm, 150mm x 125mm x 4.8 mm, 150mm x 100mm x 4.8 mm, 150mm x 75mm x 4.8mm and 150mm x 50mm x 4.8 mm for investigating the effect of laminate geometries on the contact force. From the results maximum contact force is found on 150mm x 150mm specimen. She also concluded that the mechanical behavior of the composite structures under low velocity impact is dependent on their in-plane dimensions.

From a recent study of Hosseinzadeh et al. [13], published their study in 2006 on fiber reinforced composite plates under drop weight impact who use in this study two types of glass epoxy which are categorized as thin and thick plates. All samples have same dimensions of 270mm x 270mm with different thickness. Thin glass epoxy sample has a thickness 2.4 mm. and density of 2500 kg/m^3 with a stacking sequence $[45/-45]_6$. The second sample is thick glass epoxy which has a thickness 4 mm. and has same density with the thin plate. The layer configuration of the plate is also same as the thin plate. Therefore, in this study they try to understand the thickness effect on the behavior of composite subjected to drop weight impact. The used impactors weighed 2.5 kg and 5.5 kg. The experiments were done by changing the impact energies with the levels of 30, 50 and 100 J,. All samples were clamped uniformly on all four edges (Figure 2.4). As a result of this study, the glass fiber reinforced plates with two different thicknesses failed with the smallest impact energy of 30 J.

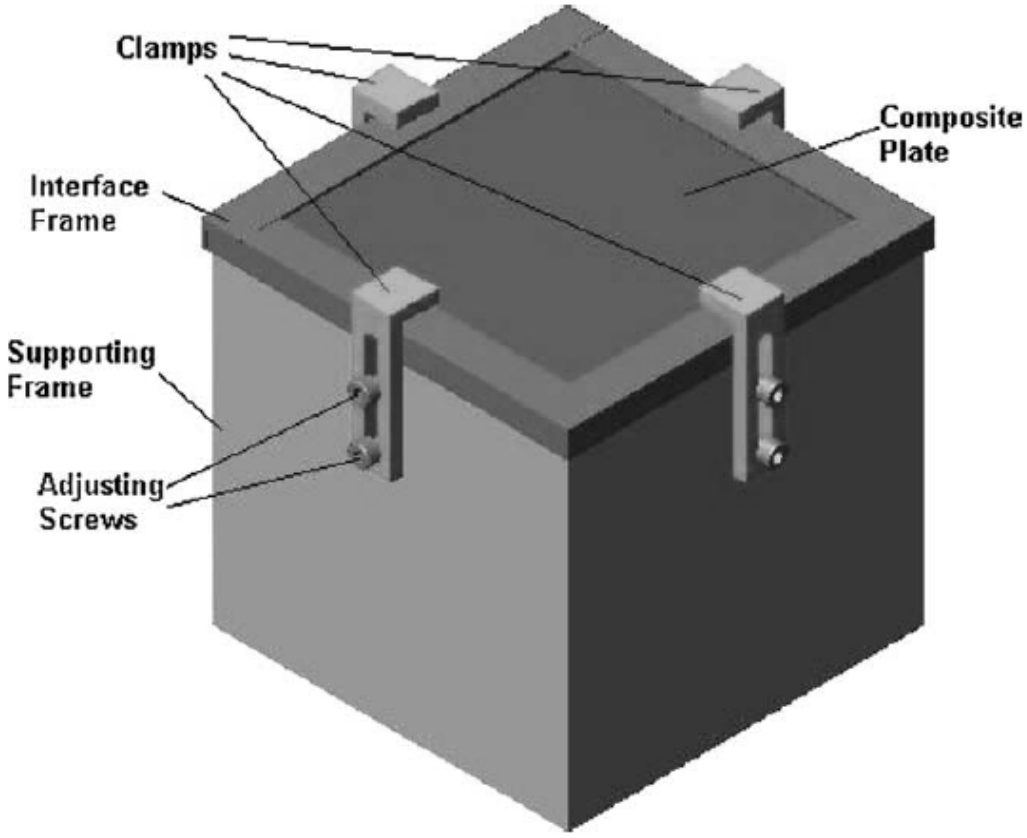

Figure 2.4 Clamped Composite Specimen [13]

In the study of Sevkat et al., [14] one of the tested specimen type is glass fabrics. Four different levels of impact is applied to the specimens with the values of 47, 60, 71, 122 J and the impact velocity values of 3.9, 4.4, 4.8, and 6.3 m/s. The used specimens' dimensions are 101.6mm x 101.6mm x 6.35mm with 55% fiber volume fraction. 37 layers of plain woven fill warp glass fabrics are produced with vacuum assisted resin transfer molding technique. The impactor has a hemispherical tip of 16mm diameter for a total weight of 6.15 kg steel (Figure 2.5). From this study's experiment the time histories of impact force and dynamic strains were recorded. From this study, glass fabrics showed low resistance to impact when they compared with the hybrid composites. The hybrid composites study of Sevkat et al., will be shown in section 2.5.

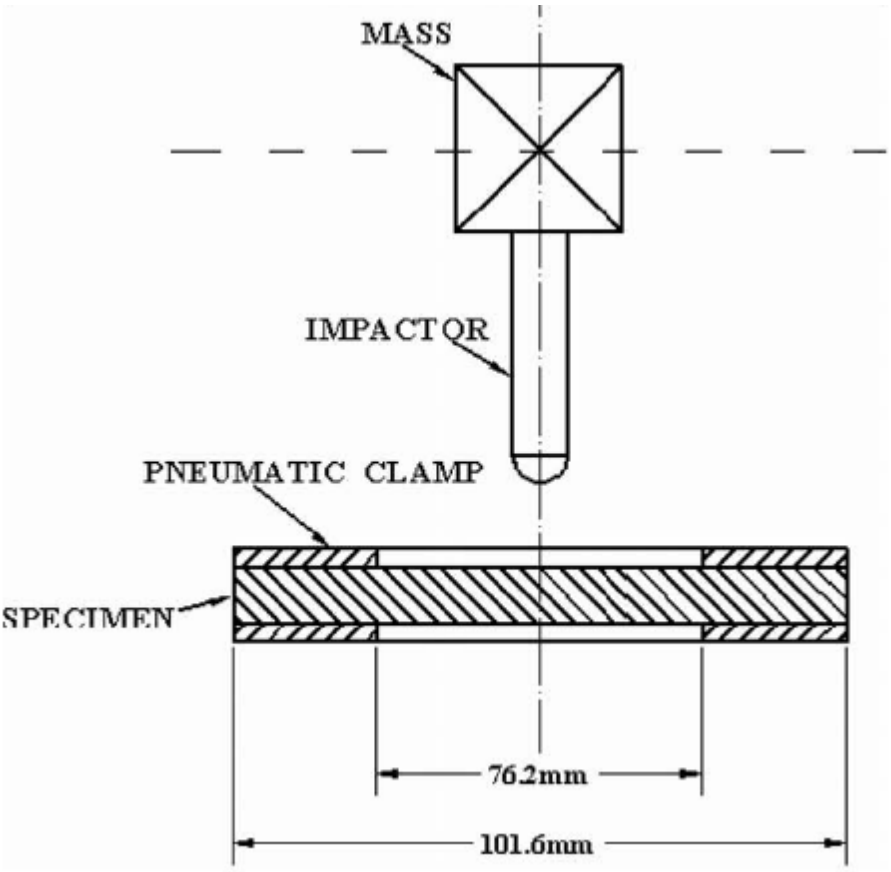

Figure 2.5 Clamped Composite Specimen From the Schematic of the Test Setup [14]

2.4 Carbon Fiber Reinforced Composite Plates under Low Velocity

In addition to fibre glass materials Naik et al., also investigated the damage to carbon fiber materials under low velocity impact. For the carbon fibre reinforced composites the same setup was used as in the fiber glass reinforced specimen experiments. The sample dimensions were 150mm x 150 mm x 6 mm. thickness and the stacking sequences were $[0/90]_s$ and $[0]_n$. The densities of the T300 carbon fiber and epoxy resin were 2620 kg/m^3 and 1170 kg/m^3, respectively. The initial velocity of the impactor was 1 m/s. The the carbon specimens were plain weave and were compared with the unidirectional samples to investigate the differences in their impact behavior. Their They compared the behavior of the material structure

using the finite element formulation.

Hou et al., [12] worked on numerical investigations of the failure criteria for laminated composite structures. Their focus was on delamination, matrix cracking and fiber failure through the specimen thickness. They used the well known Chang-Chang failure criteria [10] to solve the numerical problem. The tested specimen was unidirectional CFRP T300/914 with a volume fraction ratio of 60 %. The plate had 21 plies with a stacking sequence of [0/90]. The dimensions of the test specimen were 85 mm x 85 mm with a thickness of 2.6 mm and the plate boundary conditions were applied to a specimen supported by a support block with a diameter of 45 mm (Figure 2.6). The impactor had a steel 16 mm diameter spherical cap and a mass of 260g. The initial velocity of the impactor was 7.08 m/s. This study differed from the others in that the impact test setup was one which progressed horizontally (Figure 2.7).

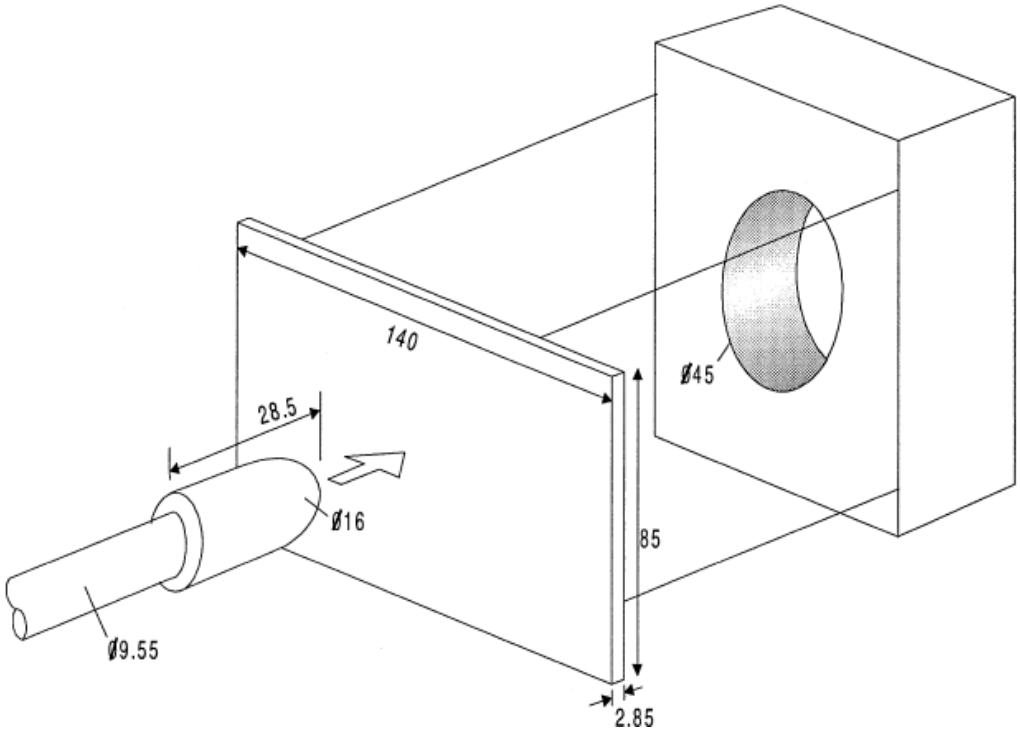

Figure 2.6 The Supporting Part of the Experimental Setup [10]

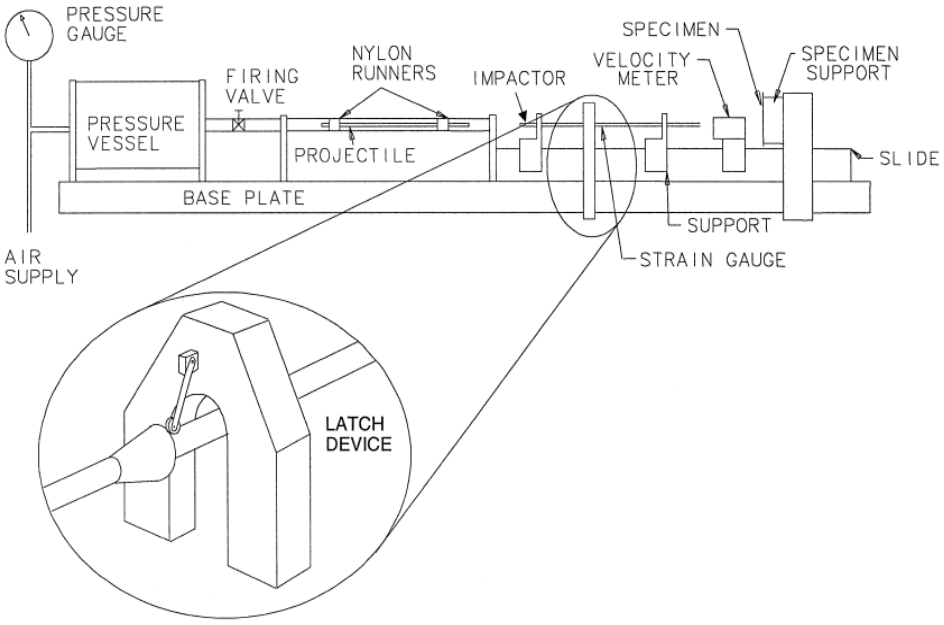

Figure 2.7 Gas-gun Experimental Test Setup Apparatus [10]

In 2003 Belingardi et al., investigated fiber glass reinforced composites [8] which concerned the laminate thickness of carbon epoxy composite plates subjected to low velocity impact by using a dart impact test setup. In this study they focused on the energy absorption capability of the carbon material and the sensitivity of its mechanical characteristics with respect to the strain-rate effects. They worked on two different stacking sequence types; $[0/60/-60]_i$ and $[0/90]_i$ with 3 different thicknesses for each stacking sequence with 4, 8, and 16 layers. The result of the experiments showed that the carbon fiber epoxy had no sensitivity in its mechanical characteristic in relation to the strain effect and the saturation of impact energy value increased with the laminate thickness.

Her et al., [2] studied T300/934 graphite epoxy laminate under low velocity impact, numerically. They used a modified Hertz contact law to calculate the contact forces analytically with loading and unloading equations. In the trial experiments, 76.2mm x 76.2mm x 2.54mm mm graphite epoxy composite laminates with a $[0/-45/45/90]_{2s}$ stacking sequence was used. A steel impactor was selected with a 6.35

mm radius and a density of 2800 kg/m3. The impact velocity was 25.4 m/s. The laminate boundary conditions were clamped and simply supported in the numerical calculations. For the failure analysis the Choi and Chang impact damage mechanism was used. In this impact mechanism, a point nose impact type was used with different composite laminates and a different impactor. The details of the first lamina were $[0_3/90_3/0_3/90_3/0_3]$ stacking sequences of the dimensions of 100mm x 76mm x 2.16 mm and for the second lamina $[0_4/45_4/-45_4/90_4/-45_4/45_4/0_4]$ with a thickness of 4.03 mm. In the experiments the specimen was clamped along two parallel edges with the other edges left free as shown in Figure 2.8. The composite lamina was impacted by a steel ball with a radius of 6.35 mm and a density of 7870 kg/m^3. The impact velocities on the both lamina were 3.22, 4, 6.7 m/s.

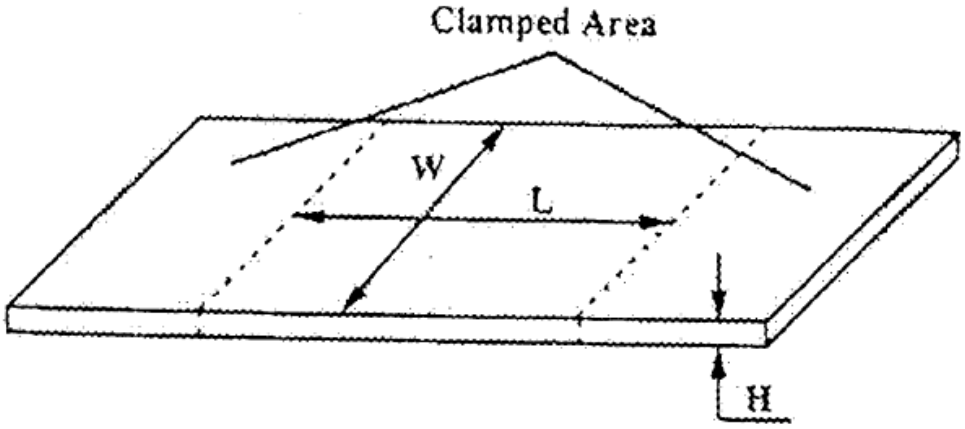

Figure 2.8 Specimen Used for Experiments and Its Boundaries [2]

Hosseinzadeh et. al., [13] also used carbon epoxy lamina with the same experimental conditions, failure criteria method and lamina dimensions. However, the thickness of the specimen was 2.8 mm and the structure of the composite was non woven long fiber property. The carbon epoxy composite specimens had a density of $1600kg/m^3$ and a stacking sequence of $[0/90]_4$. From the numerical test results carbon/epoxy showed a good structural resistance to low velocity impacts compared with the fiber glass specimens.

Sevkat et al., [14] also investigated graphite epoxy composite plates which were of the same sizes like fiber glass fabrics. However, in this specimen, the number of graphite layers was 28, with a thickness of 6.35 mm, and the density was 9.26 kg/m^2.The test setup, the shape of the impactor, production method and the impact velocities applied onto the specimen were the same as those used for the fiber glass samples. In the experiments using carbon reinforced epoxy composites the examination of damage area and absorbed impact energy of the test specimen, showed that carbon was a weak material under impact compared with the hybrid (carbon and fiber glass) specimens and fiber glass reinforced specimens

2.5 Hybrid Composite Plates under Low Velocity Impact

In addition to being produced from a single material composites can also be combinations of two or more materials [27] which is called a hybrid structure and the types are classified according to [28] as ;

- interplay or tow by tow in which tows of the two tows or constituent types of fiber are mixed in a regular or random manner;
- sandwich hybrids or in another words, core-shell, that can be defined, one material is sandwiched between two layers of another;
- intimately mixed hybrids, where the constituent fibers are made to mix randomly thus no over-concentration of any one type is present in the material;
- interply or laminated, can be defined as; alternate layers of ; two or more materials ; stacked in a regular manner;
- other types such as those that are reinforced with ribs, pultruded wires, thin veils of fiber or combinations of the above.

In the literature many of the recent investigations focused on comparing hybrid composites with single reinforced composite materials in order to understand the mechanical and impact behavior of the hybrid structure under low velocity.

Sevkat et al., [14] carried out a study on fiber glass reinforced, carbon fiber reinforced specimens and hybrid specimens. They were all plain weave woven and produced from S2 glass-IM7 graphite fibers/toughened epoxy (cured at 177 ºC) (Figure 2.9). The first hybrid specimen was designed as GL/GR/GL which contains nine layers of glass fabric face sheets with nine layers of glass fabric (GL) on each side for a total of 18 layers and 16 layers of graphite fabric. The second hybrid specimen was constructed in a similar manner but as GR/GL/GR which consists of 8 layers of graphite fabrics (GR) on each outer side and 16 layers of glass fabric in the middle (Figure 2.9). They found the best impact behavior results from the hybrid specimens. The test setup, the impact velocities applied to the specimen, the impactor and production method were the same as the fiber glass and carbon fiber samples.

Hosseinzadeh et al., [13] undertook hybrid trials on composite carbon and glass fiber reinforced plastic specimens. The composite material had a structure of a woven mixed mat long fiber in each ply with a $[45/-45/0/90/45/-45]_2$ orientation, dimensions of 270mm x 270mm x 3 mm and a density of 2150 kg/m^3. This type of hybrid composite was different from that used in the study by Sevkat's et al. The carbon and glass fibers were not located in separate plies, they were woven together to form a mixed mat in each ply. The test conditions and impactor were the same in the hybrid experiments as in those carried out on the carbon and fiber glass epoxy composite specimens. From results of the experiments, in the hybrid specimen the use of carbon and fiber glass had a positive affect on the low velocity impact and weight reduction respectively.

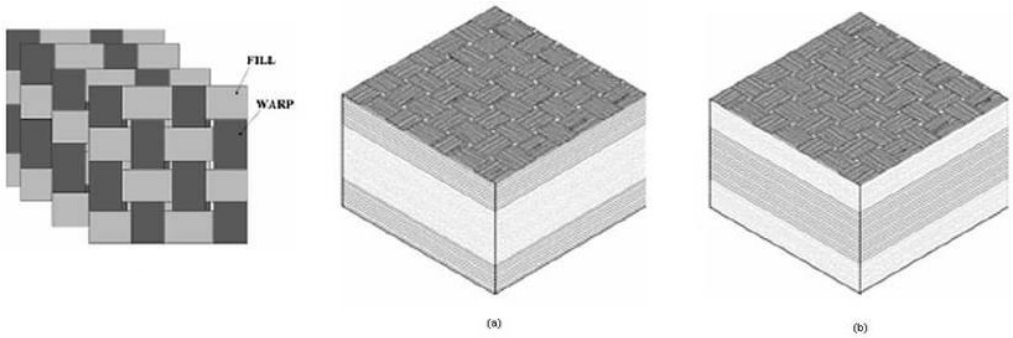

Figure 2.9 Hybrid Plain Woven Fabrics (a) Glass skin graphite core (GL/GR/GL), (b) Graphite skin glass core (GR/GL/GR) [14]

The investigation by Sayer et al., [1] in 2010 was carried out with four different combinations of hybrid composites, fabricated from unidirectional fabrics by a hand layup method. Their nominal thickness and unit volume densities are shown in Table 2.3. In the impact experiments, the applied impact energies range changed from 15 J to 65 J. The applied energy was raised until perforation took place. From the experiment results the required behavior of the hybrids in this study was perforation threshold. The aramid and carbon reinforced hybrid composites with a stacking sequence of $[0/90/\pm45]_A+[\pm45/90/0]_G$ showed a higher performance compared with other hybrids.

Table 2.3 Layer Configuration and Properties of the Hybrid Composites; A: aramid fabric, G: glass fabric, C: carbon fabric [1]

Sample ID	**Stacking Sequence**	**Nominal Thickness (mm)**	**Unit volume density (g/cm^3)**
AG1	$[0/0/90/90]_A+[90/90/0/0]_G$	2.4	1.416
AG2	$[0/90/\pm45]_A+[\pm45/90/0]_G$	2.4	1.416
AC1	$[0/0/90/90]_A+[90/90/0/0]_G$	2.7	1.407
AC2	$[0/90/\pm45]_A+[\pm45/90/0]_G$	2.7	1.407

CHAPTER 3

EXPERIMENTAL SETUP AND COMPOSITE TEST SPECIMENS

3.1 Introduction

Impact drop weight test is the main focus of this thesis. The composite specimens must be tested in order to find an optimum composite material for the pilot helmet. Therefore, research was undertaken concerning the different types of impact test rigs and this chapter contains information about the basic types of an impact drop weight test systems and composite specimens. Details are presented of the previous impact drop weight test rig in Gazi University[38], the parts that were redesigned and the mechanical properties of the composite test specimens.

Four different types of measuring equipment were used in the experiment as follows. First accelerometers which are described in relation to their use in impact drop weight testing. The measurement capacity is the fundamental criteria for the choice of accelerometer. Thus, in this study in order to satisfy the requirement in the ANSI standard (maximum 300 g acceleration value) for the protection of head from impact, the capacity of accelerometers is important. The second device is the load cell and it is the mounting type that is important because of the transmission of vibrations via the mounting on the test hammer. Ring quartz load sensors were used in the impact tests. Third the data acquisition device. This device was also used in this study to transfer the data to the software. Finally, the

optical photocells, chosen for their ease of use in measuring the time from beginning of the drop to the point of impact on the composite specimen.

The original test setup, was designed for testing the impact behavior of large civil engineering specimens Thus it had to be redesigned for use with smaller size composite specimens in order to simulate the ANSI Z90.1 1992 test standard [32], to measure the impact energy attenuation and acceleration levels on the helmet. However, there were some differences between the test rig and the ANSI Z90.1 1992 [32]. These differences are related to the shape of the test specimen and the positioning of the apparatus on the test tower.

3.2 Accelerometers

Accelerometers are generally used in absolute motion, shock and vibration measurements. The life cycle of a structure is directly proportional to acceleration intensity which is applied to it. By measuring the vibration amplitude and phase at different points of the structure a modal analysis can be undertaken. The aim of this analysis is to discover the dynamic character of the whole system through the modes of dynamic working components. High frequency accelerometers can be used in impact tests and also in high speed motor tests.

When piezoelectric elements are affected by an external force, an electric load is created on opposite surfaces**.** The piezo structure is shown in Figure 3.1 the large circles are silicon atoms and the small circles are oxygen atoms. Natural or processed quartz crystal is the most sensitive and steady state type of piezoelectric material. In addition to natural materials polycrystalline and piezoceramic materials can also acquire piezoelectric properties. These crystals produce a very high load and according to their properties, in particular, very low amplitude signals can be measured.

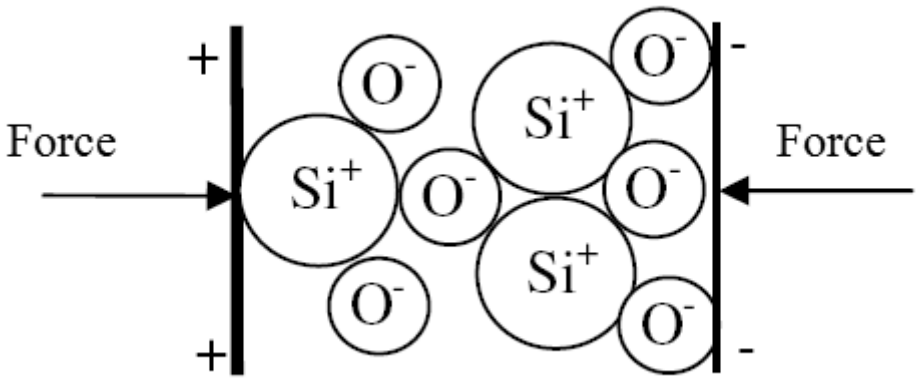

Figure 3.1 Piezo Structure [38]

The physical properties of piezoelectric material cannot change permanently and thus the piezoelectric sensors are protected by a well-supported cover. In a wide amplitude interval, for instance 120 dB, they show excellent linearity. However, piezoelectric materials can only measure dynamic cases or in other words they can measure variable cases. They cannot measure static quantities such as gravity, barometric pressure, and weight force. At the beginning these static quantities or cases are showing a signal, but this signal is annihilated as time passed because of the electric circuit's time coefficient of the connected piezoelectric material sensor. Force and acceleration sensors use piezoelectric materials because they are changing with time. Figure 3.2 shows the structure of acceleration and force sensors; the gray parts show the tested specimen, the blue parts is the sensor cover, the piezoelectric material is red , the black parts show the deformed electrodes on the crystal which the load are gathered together and the electrical load signal conversion to the voltage signal microcircuit is yellow. In Figure 3.2 accelerometers (the green part) shows the seismic mass. The force, which affects the crystals, is calculated according to Newton's Second Law of motion.

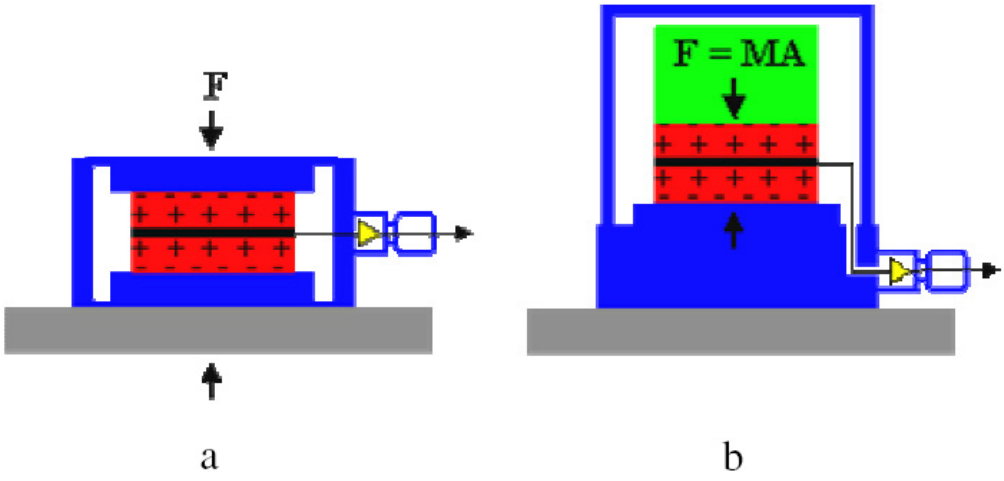

Figure 3.2 Piezoelectric Sensors a. Force Sensor and b. Acceleration Sensor[38]

3.2.1 Piezoelectric Accelerometers

Piezoelectric accelerometers are sensors, that are used in a wide range of low frequency applications. They are small and have the capability to operate in a high working temperature. The electrical load variation on the crystal of the accelerometer is directly proportional to gravity. The inertial force, which is subjected to the seismic mass acceleration on the accelerometer, affects the piezoelectric force and gives an electric signal proportional to the acceleration. In the microcircuit of the piezoelectric accelerometer, there is a signal conditioning circuit that converts the signal from the accelerometer to a voltage signal. These kinds of sensors are minimally affected by noise thus, data from the noisy and hard impact tests can be measured in an accurate way.

3.2.2 The Accelerometers used in the experiments

In this study two Integrated Circuit Piezoelectric(ICP) accelerometers were used (Figure 3.3). Their model is 353B02 from PCB™ Group,. The advantages of the ICP

type accelerometer are; constant voltage sensitivity without concern over the cable length and type, low level noise interval, data capture equipment, recorder and signal analysis. To obtain a measurement from this type of accelerometer, type of mounting is important. The characteristic properties of the mounted area, surface finishing of the specimen, temperature difference range and transportability are affected by the mounting area. In Figure 3.4 shows the mounting sensitivity of the PCB company tests, carried out under high frequency conditions.

Figure 3.3 Accelerometer 353B02 [34]

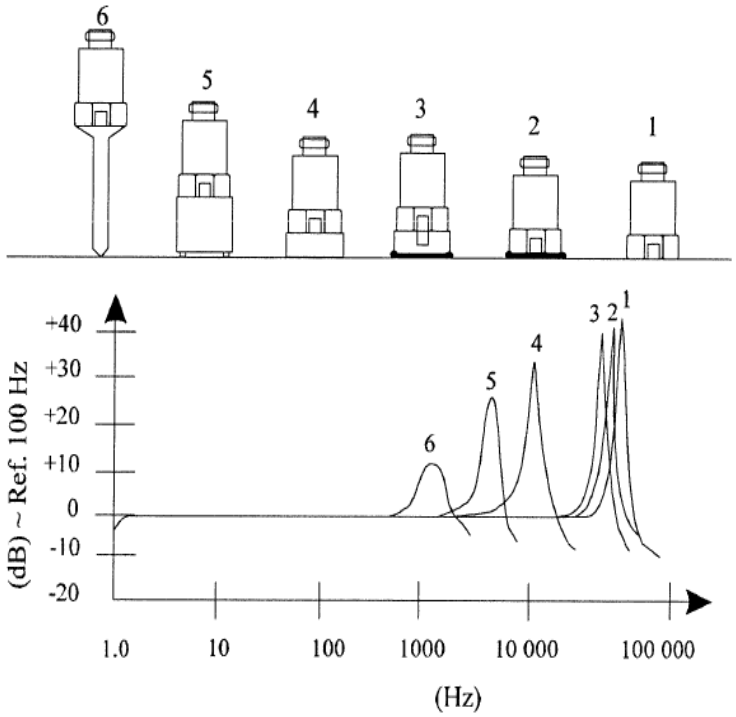

Figure 3.4 Type of Accelerometer mounting and Effects on the Frequency (1) screw (2) adhesive (3) mounting pad (4) flat magnet (5) two faced magnet (6) hand rod [38]

3.3 Load Sensor

Quartz load sensors measure tension, compression forces, impact, action and reaction forces which are strong, long lasting and dynamical usage elements. The main function of these sensors is to monitor impact forces from impact tests, mechanical impedance, penetration, vibration excitation, strength and welding operations.

The main properties of load sensors are:

- High frequency fast reaction
- Sensing large forces' signals by small sizes
- A rigidity property equal to steel

- Long lasting performance and high durability since its rigid structure
- High voltage low impedance output for ICP type sensors
- Ability to measure large static loads on small force fluctuation
- Good performance in terms of accuracy, consistancy and repeatability
- Static calibration ability and at constant temperature conditions the ability to undertake static measurements

3.3.1 Ring Quartz Load Sensors

Ring quartz load sensors are designed for dynamic pressure measurements so they can be used in force controlled affected vibrations, mechanical impedance tests and pressing works. These kinds of force sensors are appropriate for tensile stress measurements during cold forming and metal cutting processes. They have ability be statically calibrated and can undertake short time static measurement. Furthermore, they have good repeatability performance and high accuracy properties. Although the environment may have poor ambient conditions ring quartz load sensors have air impermeability thus they can be used safely.

3.3.2 The Ring Quartz Load Sensors used in the experiment

In this study model 202B ICP ring quartz load sensor from the PCB^{TM} group was used (Figure 3.5). These load sensors can be used in the same way as accelerometer sensors. The mounting type selection is important for an accurate testing stability as with the accelerometers.

Figure 3.5 Model 202B ICP Ring Quartz Load Sensor [35]

The mounting type and conditions are important because the measurement accuracy can be affected by mounting errors. Figure 3.6 shows the mounting type of the ring quartz load sensor and the technical data table of the load sensor model 202B ICP is given in Appendix B.

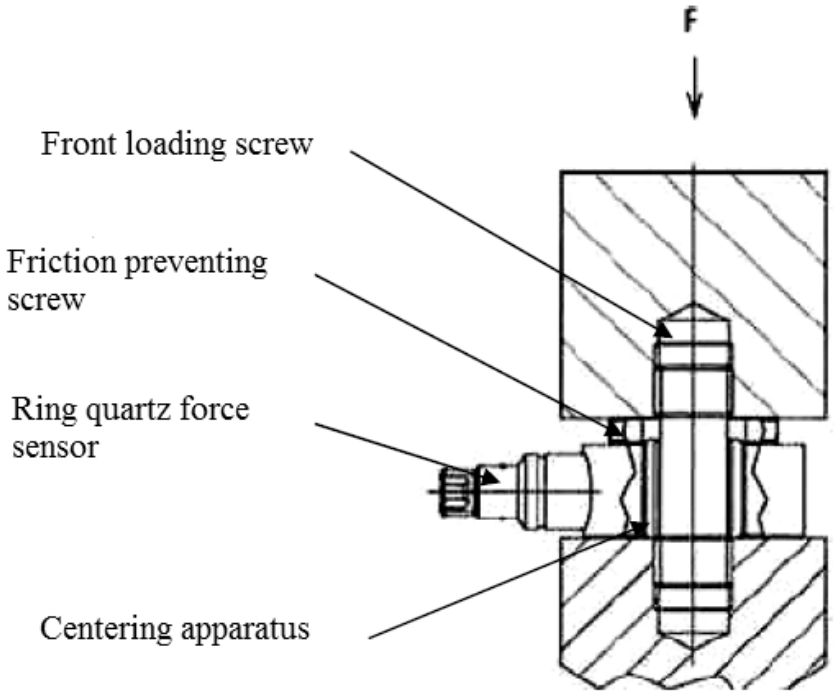

Figure 3.6 Mounting Type of the Ring Quartz Load Sensor[38]

3.4 Data Acquisition Device

The data acquisition devices are used to transfer the data from experimental

equipment to the computer storage so that it can be evaluated. They have many types both standard and specialized; and the criteria for choice of the data acquisition device is important [38] and the selection is derived from the usage area of the experiments such as the forcing effect type and the measurement tools types. Thus, in the current study, according to the testing conditions a National Instruments company device, NI™ 9233-USB-9162 model was selected.

This data acquisition device has two independent modules. The first one is used for data acquisition and is connected to the other measurement tools. The second is a signal carrier module which transports the data from the first module to the computer. The data is converted by a program written for the data acquisition device. Appendix C presents the technical properties of the data acquisition device NI™ 9233-USB-9162.

3.5 Optical Photocells

Photocells provide the motion without touching the restless body. A photocell is a type of resistor that decreases in resistance, when it is exposed to light. They are also known as photoresistors, light-dependent resistors and photoconductors. Optical photocells have high performance and improved structural design that results wider usage area. In large inductive and capacitive photocells the greatest distance between a photocell and the target body is about 60-100 mm. Optical photocells are of a small size therefore they can only control an area of a few square meters. Optical photocells can be classified according to three different sensing principles [23]:

- Emitter-receiver photocells
- Retro reflective photocells
- Diffusive photocells

In this study, diffusive photocells were used in experiment test setup[38]. The advantages of diffuse photocells are:

- they consist of only one photocell
- they cannot be contaminated or wrongly calibrated
- Translucent bodies can be sensed more easily

The optical photocells in this study were used to measure the time starting from the release of dropping weight to the point of impact on the experimental specimen. By helping the mounted body(see Figure 3.7) onto the hammer, when the hammer passes the photocell it is instantly triggered. and being connected to an electric circuit it take the measurements. From the time data obtained from the optical photocells, the energy from hammer applied to the test specimen can be also calculated using an integrations of time vs. accelerations graphs. After the integrations, time versus displacement graphs can also be determined. The calculation of the impact energy can be achieved by combining the load sensor data with the displacement data.

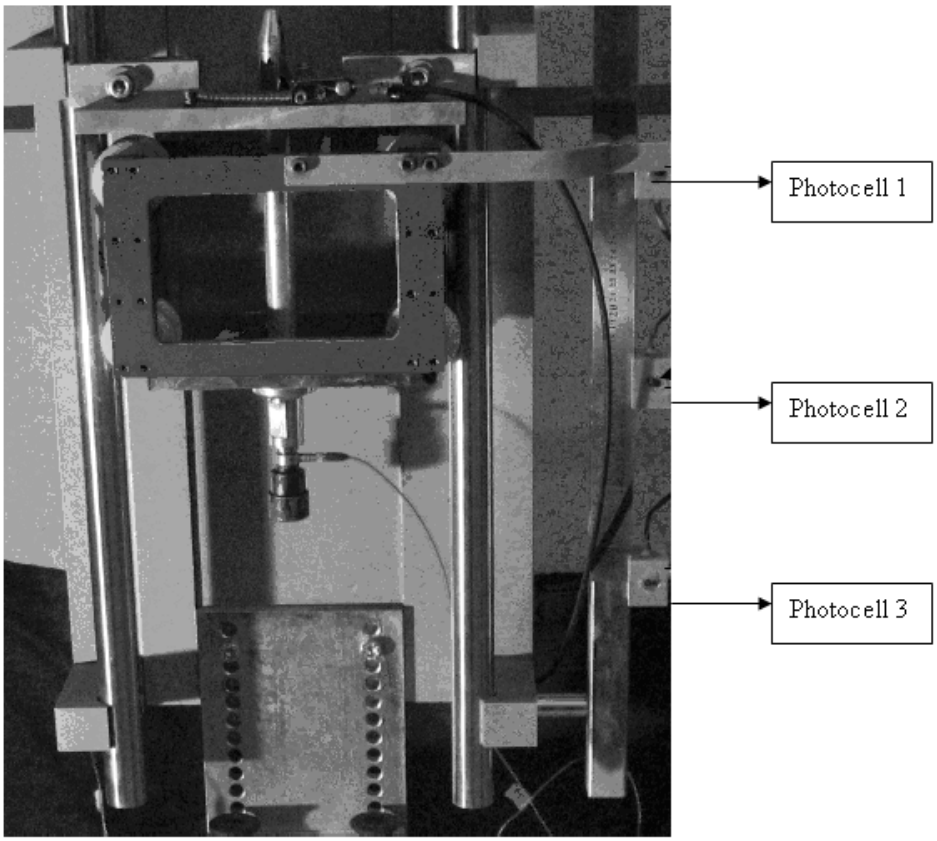

Figure 3.7 Optical photocell Locations in the Experimental Test Setup

The test setup has three optical photocells, mounted on a special slider in order to measure from the required heights (Figure 3.7). The first photocell opens the time measurement circuit when the hammer passes. The second photocell measures the first time measurement when the hammer passes. Then, the third photocell measures the total time from the first motion of the hammer to the point of impact time on the experimental specimen. Thus, the velocity versus time variation of the hammer can be measured. After this measurement has been obtained the other measurements as described in the previous paragraph and in results and discussion chapter, can be calculated.

3.6 Impact Drop Weight Test Setup

The impact drop weight test setup was chosen according to the results of the literature survey and the ANSI standard requirements. Modern test setups are different from many of those referred to in the literature since they use improved devices and methods, including sensors and computer software. This test setup used in this study has similarities with the work of Aslan [15] and Hosseinzadeh [13]. Due to the requirements of the ANSI standard the orginal impact drop weight test setup from Gazi University was redesigned using information gained from the literature review. Aslan et al., used strain gauges and MATLAB program according to the requirements of their experiments. They tried to determine the effect of in-plane stress of composite plates under low velocity impact. Hosseinzadeh et al., used computer analysis to demonstrate the impact drop weight test setup. They also used an impact drop weight and a specimen holder to determine the damage shape of the composite specimens after low velocity impact. The impact drop weight test setup in Gazi University Civil Engineering Laboratories was redesigned for impact testing of the type undertaken in this study Figures 3.8 and 3.9). The details of the redesigned parts were determined after defining the size of the test specimens.

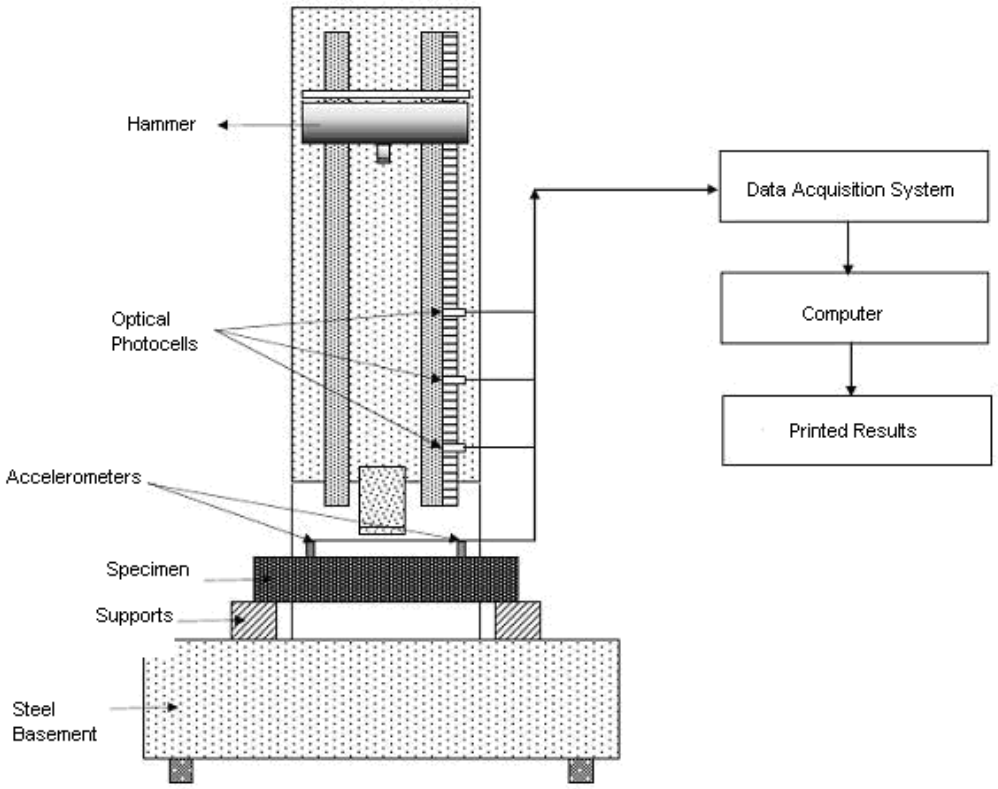

Figure 3.8 Schematic View of the Drop Weight Impact Test Setup[38]

The dimensions of the test specimens and the protection distance of the accelerometers (located on the composite test specimen) were determined. After defining the specimen dimensions as 220x220x t mm (t being between 0.82 to 2.82 mm), the specimen holder housing was designed.

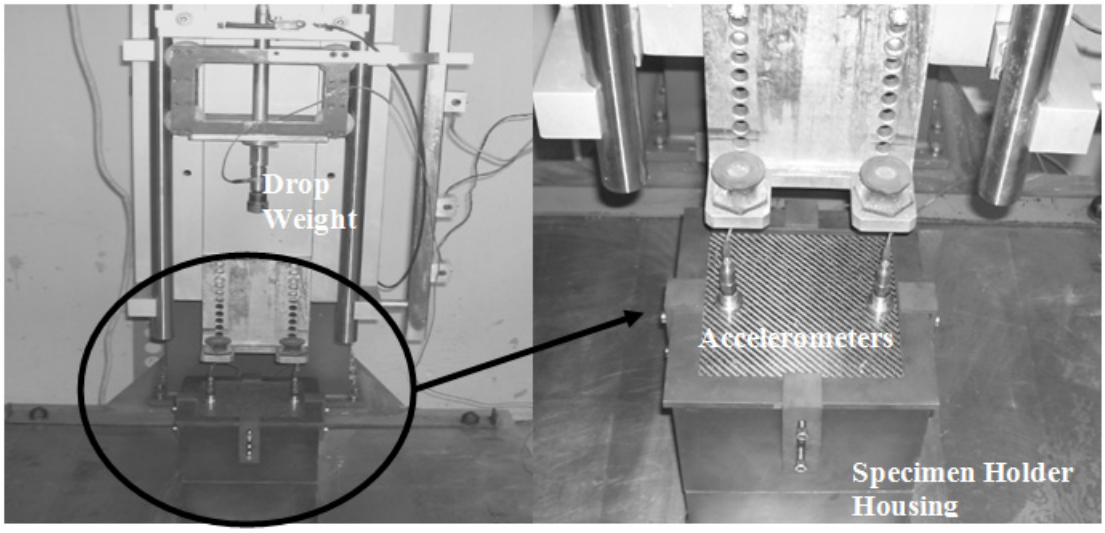

Figure 3.9 The Redesigned Test Rig with the Specimen Holder Housing

The drop weight test setup supports the energy conservation law that potential energy is transformed to kinetic energy at the point of impact. This energy conversion creates a very rapid stress accumulation on the test specimen [38].
The statements below should not be altered that a drop weight test setup can be used for impact effects observations;

- The interaction load between the hammer and specimen is not a type of bending load which comes from internal effects.
- After the occurrences of the internal loads the acceleration distribution throughout the specimen can be determined.
- According to the energy conservation law, the energy loss during falling is equal to the gain energy from experiment specimen.

3.6.1 Specimen Holder Housing

The previous setup was designed to test concrete structures for civil engineering studies, thus the specimen holder was too large for 220 x 220 x t mm specimens

and lacked the appropriate fastening interfaces . Therefore the set up was redesigned and a specimen holder of an appropriate size for the composite specimens was added.

This part of the experiment setup has four sub parts; the bottom housing, top housing, specimen holder on the top housing and four clamps to fasten the specimen holder and specimen to the top housing (Figure 3.10). The connection of the clamps to the top housing connected by screws. The height of the specimen holder can be changed by sliding the screw along the slots of the clamps. All of the parts are made from steel to prevent vibration.

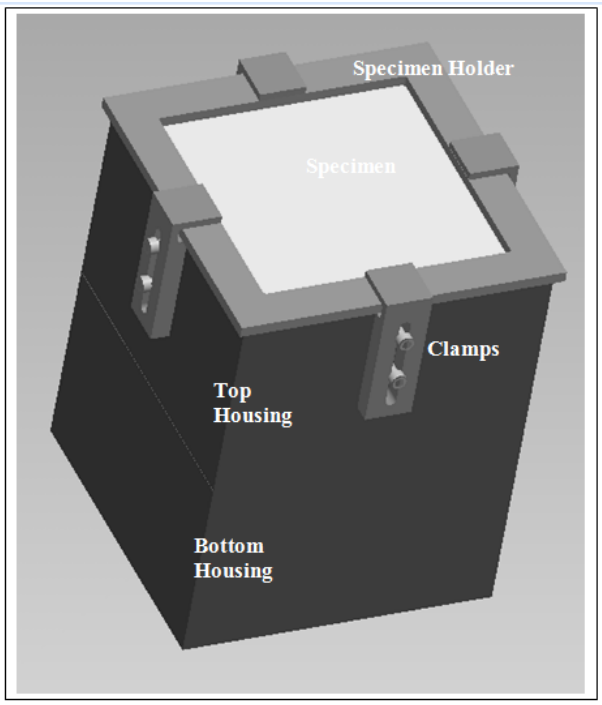

Figure 3.10 Design of the Specimen Holder Housing for the Experiment Setup

3.6.2 Drop Weight

The drop weight, made from Aluminum and weighing 5.25 kg, was used to apply the impact to the test specimens. The weight can be increased by adding weight to the hammer which is secured by a screw system. To prevent the drop weight creating friction, chrome coated rails were used, and the four edges of the internal

parts of the drop weight rail wheels were made from kestamid.

The tip of the drop weight was changeable; therefore it is possible to see the impact damage area and the damage effects at the impact point with other tip shapes of hammer. The drop system of the hammer was designed mechanically, thus the drop height of the experiment can easily be manipulated as shown in Figure 3.11.

The free fall motion of the hammer is encouraged by the chrome shafts which were 2500 mm in height and 30 mm in diameter. They were fastened to the experiment tower and their height could be increased if required. The distance between shafts was 200 mm.

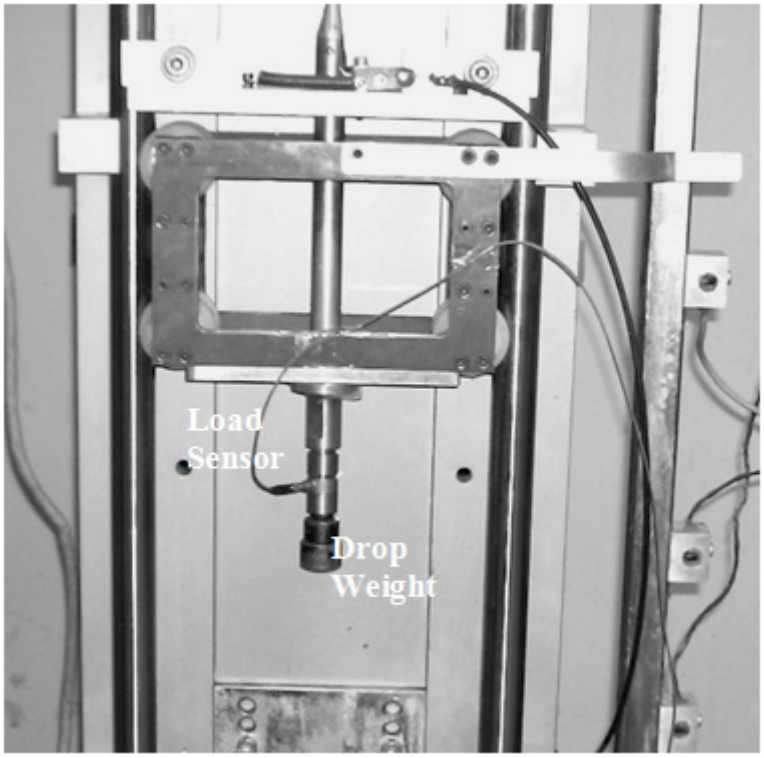

Figure 3.11 The Drop Weight and its Mechanical System

3.7 Composite Test Specimens

The structural design of the composite test specimens was achieved with information of literature review as reported in Chapter 2. The expected basic criteria from the test specimens is impact resistance, after the given impact energy. Aramid, fiber glass and carbon fibers are selected according to their mechanical properties and impact damage behaviors. The manufacturers' advice was also taking into account in the selection of the matrix and the fiber parts of the composite test specimens. The test specimens were manufactured to a thickness of 0.82 to 2.82 mm. in order to fulfill the lightweight design criteria of helmet shell. The shell thickness of commercial helmets were measured to find a thickness interval. A $[0/90]_i$ stacking sequence was chosen, because starting the structural design from a simple orientation is necessary to understand the results of the experiments. Furthermore, using different stacking sequences can be more complicated than a constant stacking sequence to compare the impact results of the experiment. However, other configurations could be tried in future experiments.

For the trial experiment specimens Sicimon® Epoxy resin SR 8500 was selected, this is a cold cure epoxy system and Araldite® LY 5052 is chosen for the test specimens. Table 3.1 summarizes the properties of the tested specimens in pilot experiments before those used in the actual experiments given in Table 3.2. The fiber volume fraction ratio was calculated for each specimen according to equation 3.1 and this is also shown in Table 3.2.

$$v_f = \frac{W_f / \rho_f}{W_c / \rho_c} \tag{3.1}$$

Where;

v_f : Volume fraction of fibers

W_f : Weight of fibers

ρ_f : Density of fibers

W_c : Weight of composite

ρ_c : Density of composite

The specimens (TCS and TGS) for the trial experiment were prepared by a vacuum bag molding process at a temperature of 20ºC with 40% humidity, and then they were vacuumed at -0.87 bar level for 24 hours with a curing finishing process However, a post curing operation was not undertaken.

Table 3.1 The Specimen used in the Trial Experiment

EPOXY SYSTEM	SPECIMEN TGS	SPECIMEN TCS
Fiber Type	GTW	CTW
Mixing Ratio of Epoxy	100/35	100/35
Density of Epoxy (kg/m3)	1.176	1.176
Density of Fiber (gr/m2)	240	290
Volume Fraction of Fibers	0.5	0.5
Stacking Sequence	$[0/90/-45/+45]_4$	$[0/90/-45/+45]_4$
Thickness	1.90	2.40

The composite specimens that are carbon reinforced, aramid reinforced and hybrid (C1, C2, A1, A2, H1, and H2) were also prepared by a vacuum bag molding process at a temperature of 20 ºC temperature with 40% humidity. They were vacuumed at -0.95 bar level with a 4 hours per 80 cycle curing process, however, again the post curing operation was not carried out.

Table 3.2 Tested Specimens

EPOXY SYSTEM	SPECIMEN C1	SPECIMEN C2	SPECIMEN A1	SPECIMEN A2	SPECIMEN H1	SPECIMEN H2
Fiber Type	CTW	CTW	APW	APW	CTW+APW	CTW+APW
Mixing Ratio of Epoxy	100/38	100/38	100/38	100/38	100/38	100/38
Density of Epoxy (kg/m3)	1.106	1.106	1.106	1.106	1.106	1.106
Density of Fiber (g/m2)	320	320	220	220	263	260
Volume Fraction of Fibers	0.62	0.60	0.67	0.72	-	-
Stacking Sequence	$[0/90]_4$	$[0/90]_8$	$[0/90]_4$	$[0/90]_8$	$[0/90]_7$	$[0/90]_5$
Thickness(mm)	2.13	2.82	0.82	2.53	2.33	1.48
Weight(g/mm^2)	1.415×10^{-3}	2.933×10^{-3}	1.043×10^{-3}	2.024×10^{-3}	2.045×10^{-3}	1.487×10^{-3}

The experimental setup is reported by comparing its properties with the literature survey's experimental setups for low velocity impact tests. After modifying the original test rig the optimum sensors were chosen acccording to the test specimen, hammer geometry and ANSI standard test requirements.. The working principles of the accelerometers, load sensors and optical photocells were examined. From the measurements from these devices graphical data for the impact energy was determined, which will discussed in Chapter 4. The properties of the composite specimens have been also summarized together with the reasons for choosing these specimens in relation to orientation, thickness and material. The test procedure and the results of the impact drop weight tests will be examined in the next chapter.

CHAPTER 4

RESULTS AND DISCUSSIONS OF THE EXPERIMENTAL STUDY

4.1 Introduction

In this study the low velocity impact duability of the composite test specimens were examined after impact damage. This impact was supplied by an experimental impact drop weight test setup which was a modified version of rig that was used in Gazi University Civil Engineering Laboratories to investigate the impact damage on concrete beams with composite reinforcements. As stated in Chapter 3 a specimen holder for the composite material was added to the original test rig .

Trial test specimens were used as a calibration component for the experimental components of the impact drop weight test setup including the accelerometers, load cell and the drop height of the hammer. The technical details of the trial test specimens and the other test specimens are summarized in this chapter. After the trial experiment study, the other composite specimens were tested.

For the trial experiments fiberglass and carbon epoxy specimens are chosen and their composite properties are shown in Table 3.1. These materials were selected on the basis of the information found in the literature review [1-18]. At the beginning of the research there was a limited aramid material in the stock held by the manufacturer (CES Industry Inc.) however, later in the experimental program

aramid was tested. Properties of composite specimens such as stacking sequences, fiber volume fraction ratios and thicknesses were defined in this study. The reason for being manufactured these test specimens' thicknesses as 1.9 mm and 2.4 is that this is the thickness used in commercially available helmets. Therefore, in order to protect the test components (especially the accelerometers and load cell) and to ensure the accuracy of the measurements, the trial test specimens were manufactured from thicker materials. However; a military helicopter helmet should be thinner than these values. Because of the other heavy weighted parts on it. The other specimens that are used in tests were manufactured in thinner heights which will be reported in section 4.4.

The 1.9 mm fiberglass epoxy trial test specimen was tested from 20 cm then 40, 80, 100 and 150 cm drop heights. The distance between two accelerometers is 12.5 cm and accelerometers were mounted on brass parts, which are attached to the holes drilled into the specimen. The second trial test specimen consists of 2.4 mm thick carbon fiber epoxy, this was tested with the same accelerometer spacing as the fiberglass. However, due to the brittle structural properties of the carbon, the drop height for this specimen was carried out at lower drop heights than the fiberglass specimen starting at 40 cm and continued up to 60 and 80 cm.

From the trial tests, some experimental problems were discovered. The first problem was the location of the steel specimen holder that was welded to the steel base of the impact test setup. As shown in Figure 4.1 it should be aligned with the hammer in order to hit the center of the specimen.

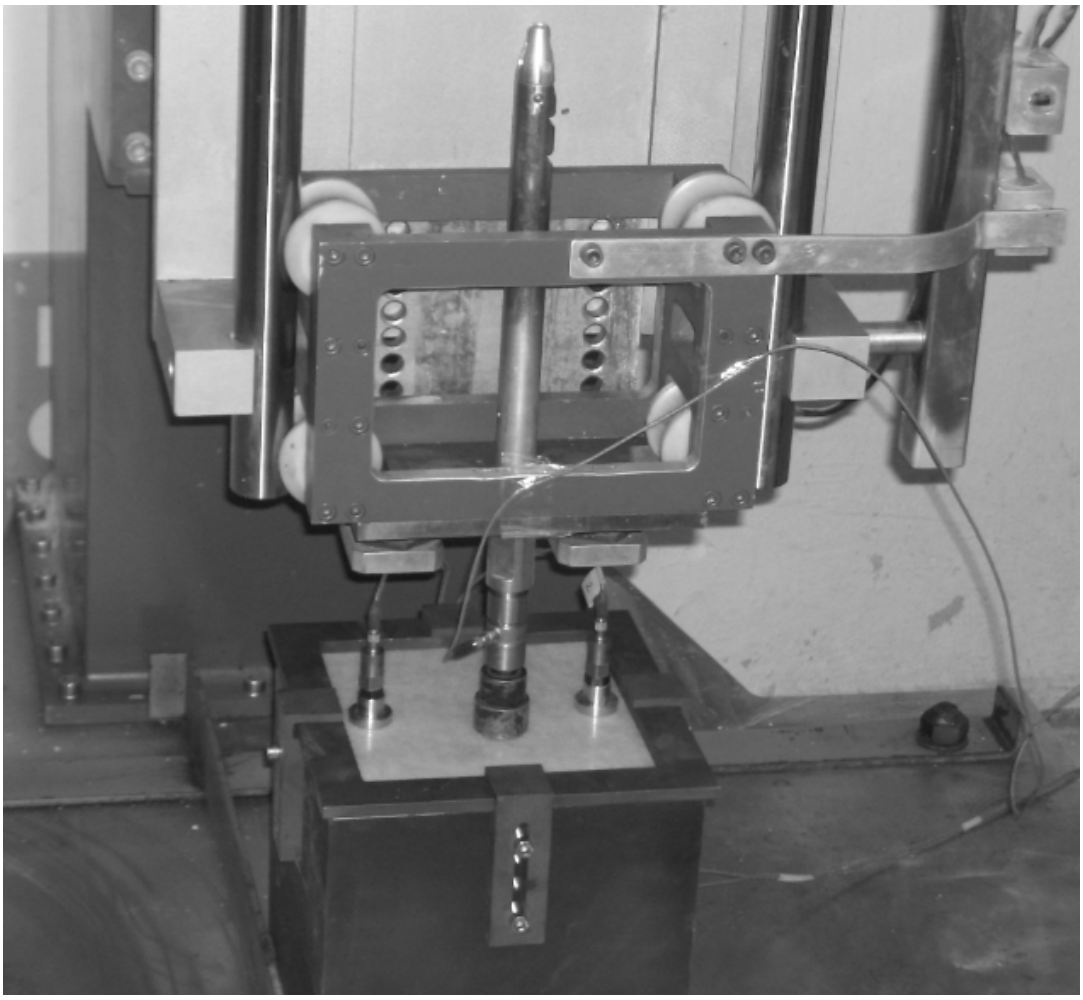

Figure 4.1 Location of the Steel Housing

Second issue was the location of the accelerometers which were close to the clamp but were far from the point where the hammer hits the specimen and thus the acceleration reading could be affected by the accelerometers locking. Therefore, it was decided that in another trial experiment the spacing between the accelerometers was narrowed to 8.5 cm and two more experiments with glass and carbon fiber epoxy specimens were undertaken. Unfortunately, the locking of the accelerometers occurred again, thus the cause was not the distance between accelerometers. Because they locked at 80 cm for the fiberglass specimen, at 40 and 60 cm for the carbon fiber test specimen. For higher drop heights acceleration level will increase. Therefore, there is a constraint on the impact drop weight experiment of this study

which is that the accelerometers can only read the acceleration up to 556 g before locking.

4.2 Experimental Test Procedure

After orienting aligning the redesigned parts to the setup the trial test specimens were used to calibrate the sensors and alignment of the parts. After the calibration procedure that was described in the previous section, the tests were carried in the following stages:

1) Accelerometers were mounted to the test specimen
2) Test specimen was placed in the specimen holder housing
3) Load sensor was mounted onto the drop weight
4) The cables from the load sensors and accelerometers were connected to the data acquisition device.
5) Computer system was connected to data acquisition device.
6) The height of drop was increased according to the predetermined height
7) Software program was started
8) After all these steps, the braking mechanism was released to drop the hammer onto the test specimen.
9) The data measured by the photocells, load sensor and accelerometers was transferred to the software by data acquisition device.
10) DIADEM software was used for checking and reading the data after the test completed.
11) The test procedure was repeated for each test specimen.

4.3 Results of the Trial Experiments

In the trial experiments, the drop height was determined for the different materials (carbon and fiber glass reinforced composites) by observing when visible damage occurred but did not cause the accelerometer to lock. Furthermore, the logged data was collected in order that graphs could be drawn by the software. Although the data logger recorded 270,000 data; unfortunately EXCEL which was initially chosen does not have the capacity to process this amount of data. Thus, another program namely DIADEM was used to process the data from accelerometers and load cell after the impact of the hammer.

4.3.1 Fiber Glass Epoxy Specimen (TGS) Results

The 1.9 mm. fiber glass epoxy specimen was tested and the results are summarized in Table 4.1and the selected acceleration time graphs for the first and the last drop heights are shown in Figure 4.2 and 4.3 respectively.

Table 4.1 Selected Results for the Fiber Glass Epoxy (TGS) Specimen

Drop Number	Drop Height (cm)	Maximum a_0 (g)
1	20	71.59
2	40	117.92
3	80	167.12
4	100	173.02
5	150	553.72

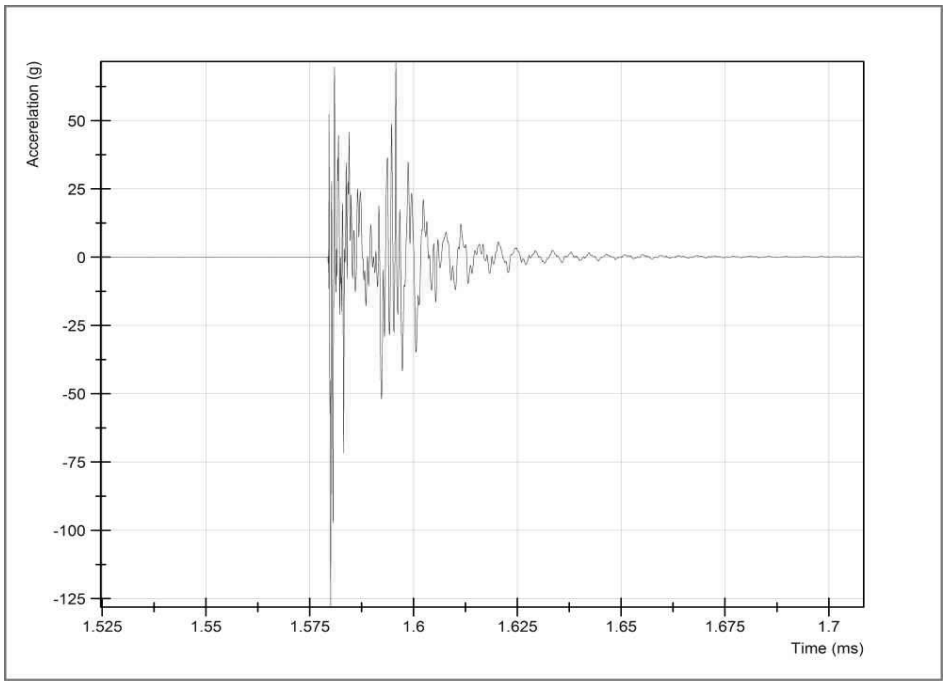

Figure 4.2 Time vs. Acceleration Graph of the First Drop for the TGS Specimen

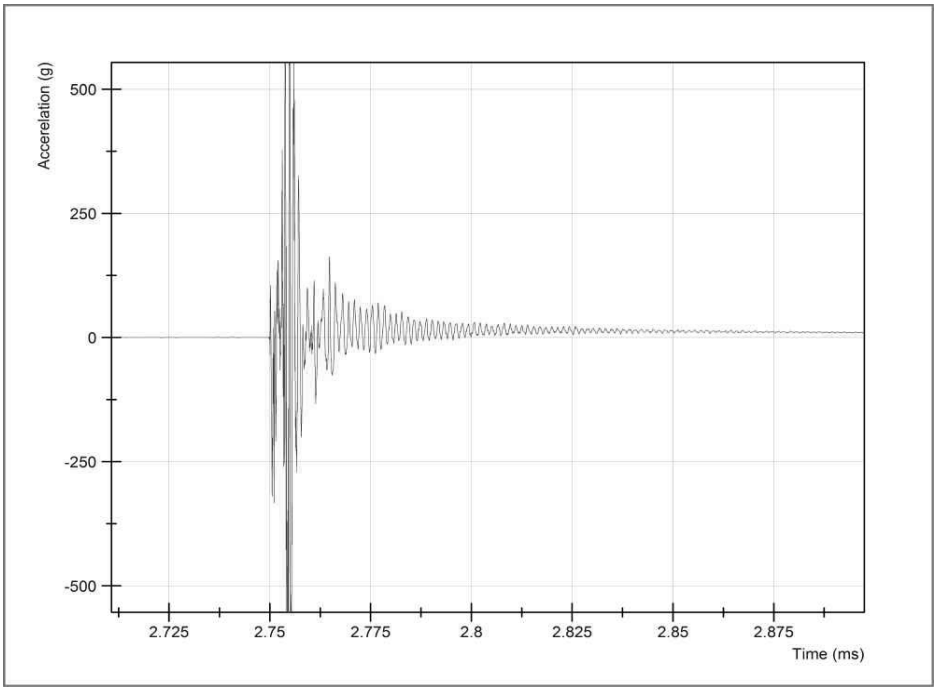

Figure 4.3 Time vs. Acceleration Graph of the Fifth Drop for the TGS Specimen

As seen in Figures 4.2 and 4.3 an increase in the drop height of the hammer caused also an increase in the acceleration. From the literature, it is known that when the acceleration value is lower then the risk of damage is also less [33]. The measured values of accelerations for the test specimens is important for the capacity of impact absorption. The impact absorption capacity of the specimens can be obtained from the calculation of the areas on displacement vs. impact load graphs. These calculations were carried out for the tested specimens and are given in Section 4.4.

4.3.2 Carbon Fiber Epoxy Specimen (TCS) Results

The second trial was carried out on the 2.4 mm. carbon fiber epoxy specimen from three different (20, 40, 60 cm) drop heights. The measurement data is summarized in Table 4.2. Furthermore, the selected time vs. acceleration graphs of the first drop height and the last drop height are given in Figures 4.4 and 4.5, respectively.

Table 4.2 Selected Results for the Fiber Glass Epoxy (TGS) Specimen

Drop Number	Drop Height (cm)	Maximum a (g)
1	20	553.73
2	40	553.73
3	60	553.76

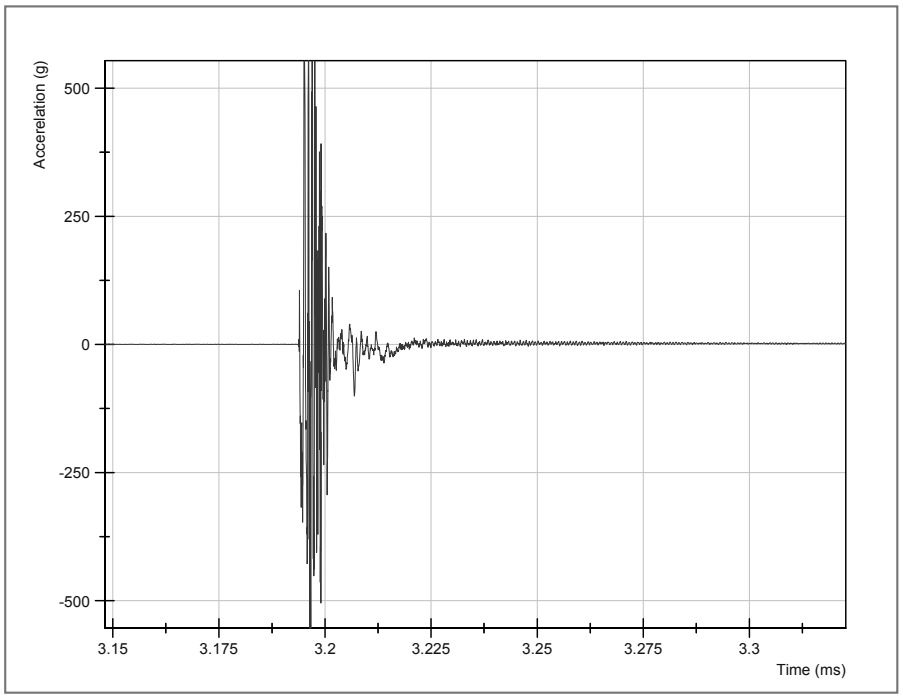

Figure 4.4 Time vs. Acceleration Graph of the First Drop for the TCS Specimen

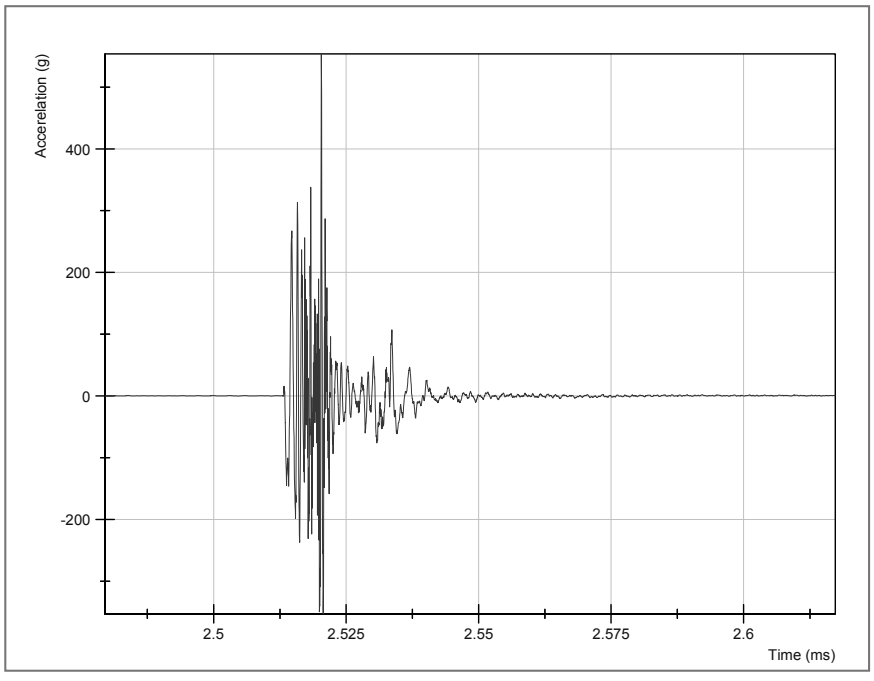

Figure 4.5 Time vs. Acceleration Graph of the Third Drop for the TCS Specimen

Figures 4.4 and 4.5 show that the increase in acceleration is not very clear in comparison with fiberglass. However, the acceleration values of the carbon fiber

composite specimen are much greater than the fiberglass epoxy specimens.

4.4 Results of the Tested Specimens

The specimens were tested according to the defined test conditions and calibrations obtain from the results of the experiments carried out on the trial specimens. From the beginning of the study the height of the drop was considered to be a constant parameter. After obtaining the results of carbon and fiber glass epoxy trial test specimens it was decided that the fiber glass reinforced specimens would not be used. The reason for this is that The density of the fiber glass is high and therefore it does not confirm the weight criteria for the helmet for a helicopter pilot. From these observations the aramid and carbon material was chosen for testing.

After the impact drop weight tests, the acceleration data of the tested specimens was collected and drawn by DIADEM. Table 4.3 shows the maximum acceleration values of the C1, A1, C2, A2, H1 and H2 specimens. Figures 4.6 to 4.9 show the time vs. acceleration, time versus velocity, time versus displacement and time versus force graphs, at a 30 cm. drop height for the H2 specimen. The rebound of the hammer is seen in the figures because there is no catching mechanism. The time vs. acceleration graph was integrated to obtain the time vs. velocity graph. After this stage, the second integration was carried out to obtain the displacement graph. The time vs. force graph was drawn by using the load cell collected data directly.

Table 4.3 Selected Results for the Specimens

Specimen Name	Drop Number	Drop Height (cm)	Maximum a (g)
C1	1	30	413.93
A1	1	30	126.34
	2	50	141.84
	3	70	242.90
C2	1	30	317.80
	2	50	418.15
A2	1	30	164.04
	2	50	202.82
	3	70	445.81
H1	1	30	212.62
	2	50	372.87
H2	1	30	96.53
	2	50	327.08

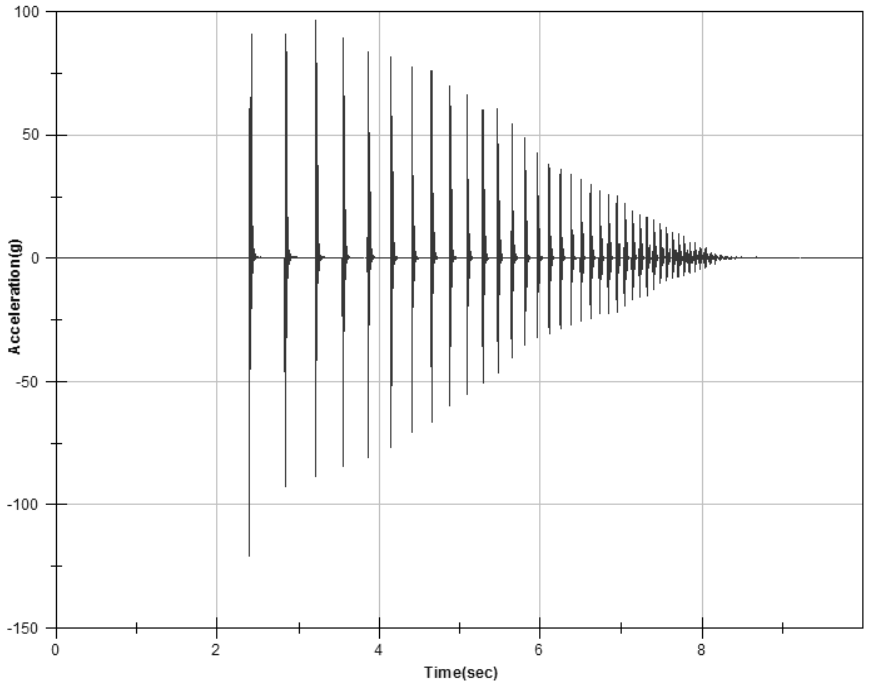

Figure 4.6 Time vs. Acceleration Graph for the H2 Specimen

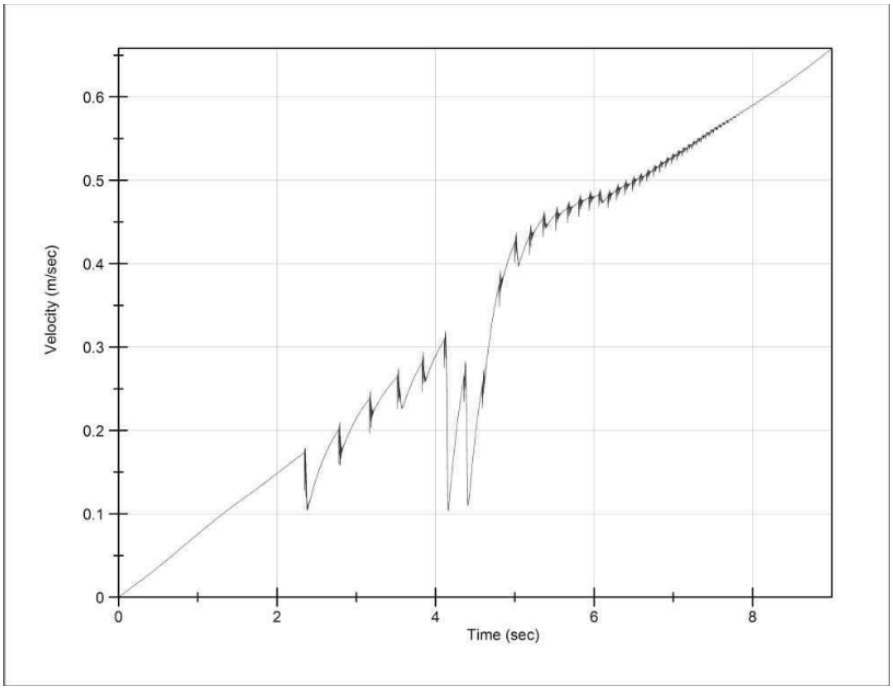

Figure 4.7 Time vs. Velocity Graph for the H2 Specimen

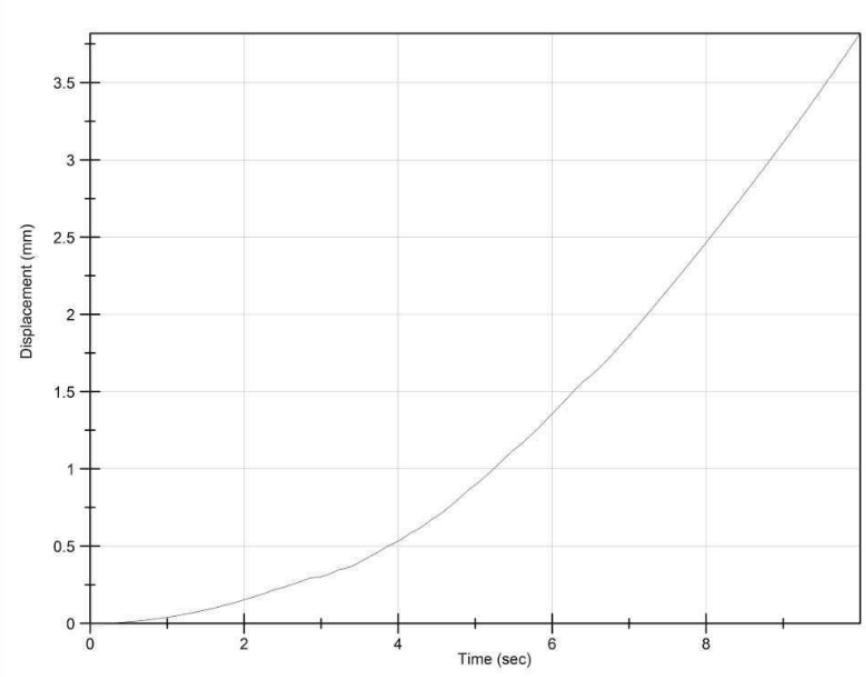

Figure 4.8 Time vs. Displacement Graph for the H2 Specimen

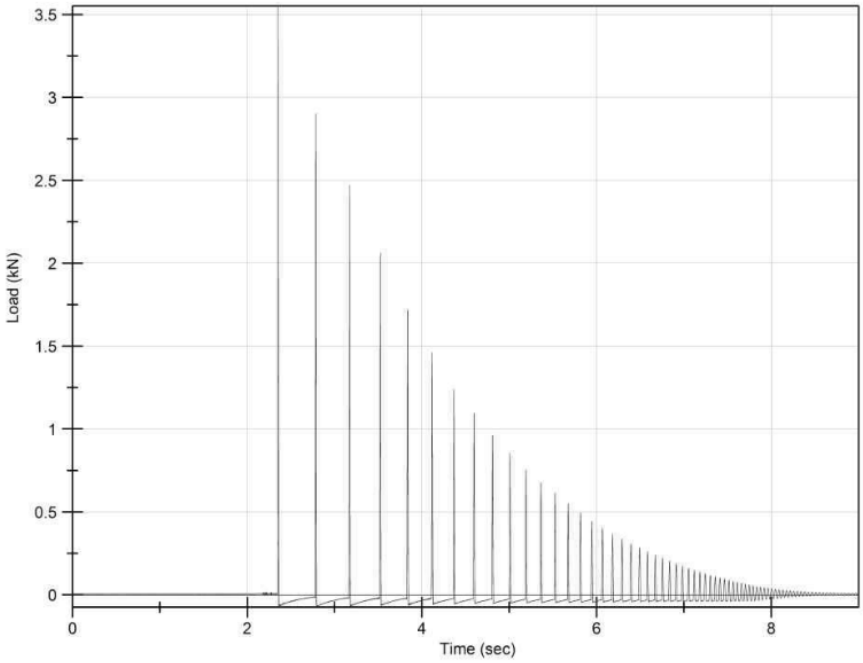

Figure 4.9 Time vs. Load Graph for the H2 Specimen

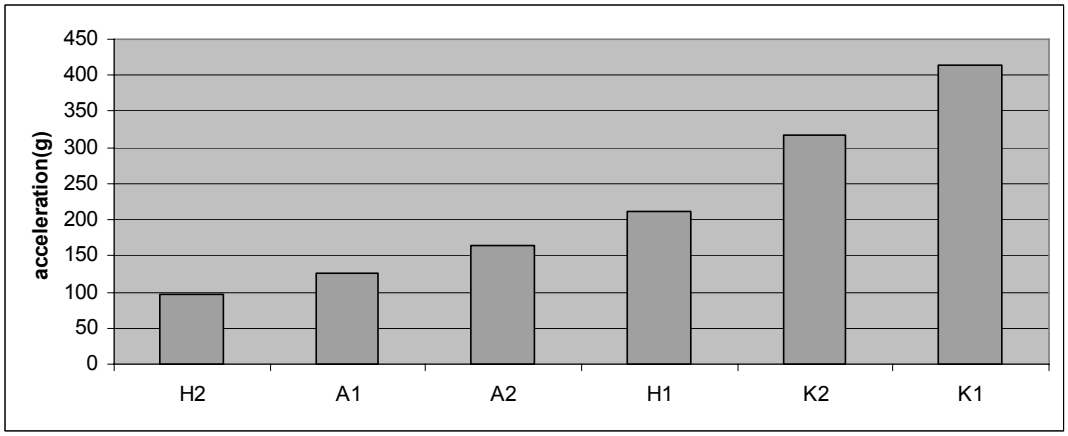

Figure 4.10 Maximum Acceleration Values for the 30 cm Drop Height for Composite Specimens

As can be seen in the Figure 4.10, the performances of the specimens are from best to worst as follows; H2, A1, A2, H1, C2 and C1. Hybrid specimens give a better

performance with the properties of carbon and aramid. Aramid absorbs less epoxy, therefore the aramid reinforced specimens are lighter and more ductile in comparison to the carbon reinforced plates. The hybrid specimen H2 has an even better performance acceleration value than the H1 hybrid composite specimen. H1 consists of four carbon plies and three aramid plies. H2 has three aramid plies and two carbon plies. The H1 specimen has more carbon plies, therefore it absorbs more epoxy. Its impact absorption capacity is lower than H2, A1 and A2 . Furthermore, carbon should be used to manufacture a helmet, because when a hole is drilled on the helmet, the edges of the aramid fiber become fuzzy (Figure 4.11). On the other hand, carbon fiber reinforced composites are expected to have worse results under impact and the experimental results proved this to be true. Although a constant height was established as 30 cm, the higher drop heights of the impact test are also given in Table 4.3. In order to determine the maximum acceleration capacity of the A1, A2, H1, H2 and C2 specimens, a higher drop height was applied and the results supports the fact that increasing the drop height will increase the acceleration level.

The damage results of the six tested specimens are shown in Figure 4.12. The damage after impact to the non impacted side damage for each specimen can be clearly seen. The C1 and C2 carbon fiber reinforced specimens, have a more brittle structure than A2, H1 and H2. A1 is the thinnest specimen and the appearance of the damage is different, since there are cracks on the both sides of the specimen. Also H1 and H2 show similar characteristics in the damaged area.

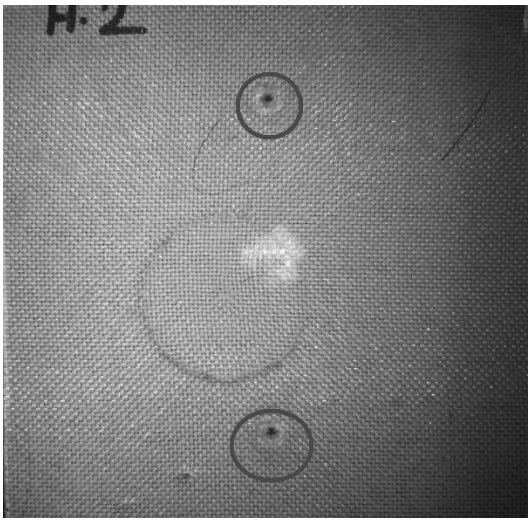

Figure 4.11 View of the holes drilled into the Aramid Specimen

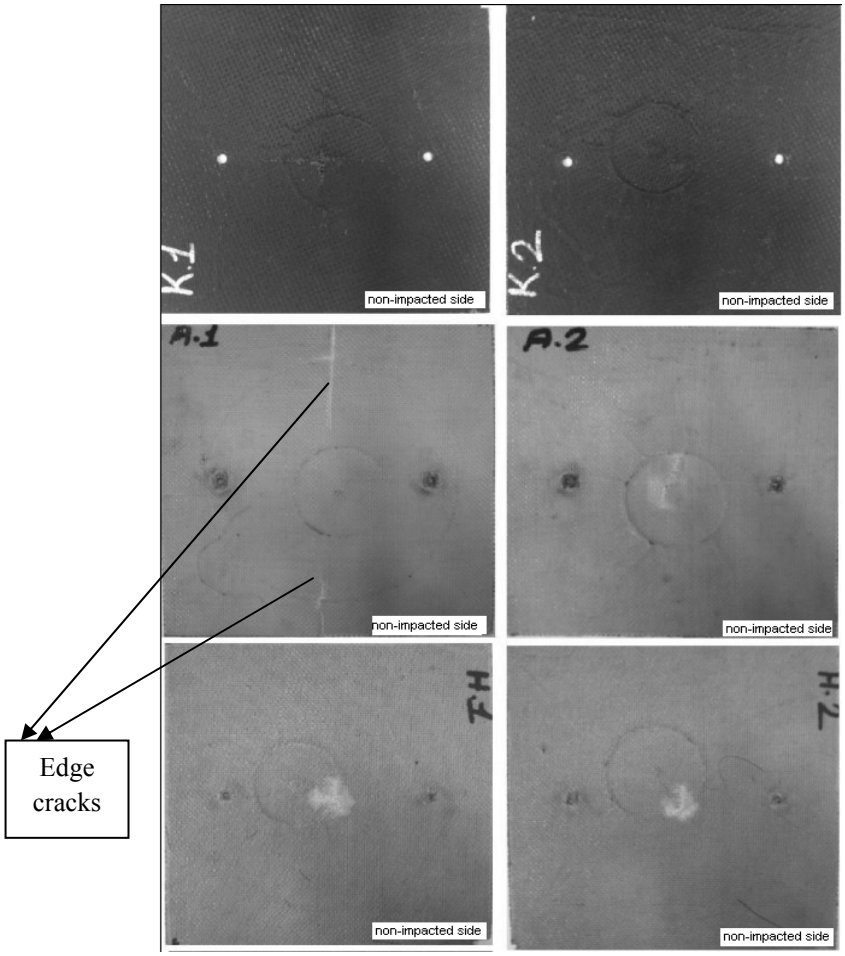

Figure 4.12 Damage Areas for Non-Impacted Sides of the Tested Specimens

After examining the acceleration values, load versus displacement graphs are used to calculate the impact energy values of the specimens. 30 cm drop height displacement load diagrams (except experiment 1) are shown in Figures 4.13 to 4.17.

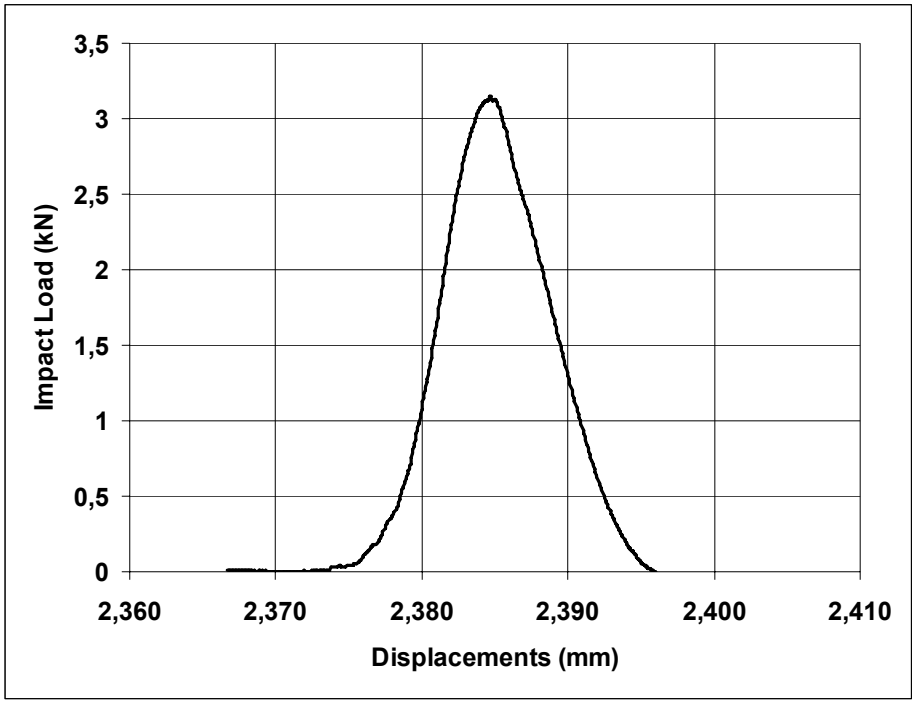

Figure 4.13 Displacement versus Load Diagram for Specimen A1

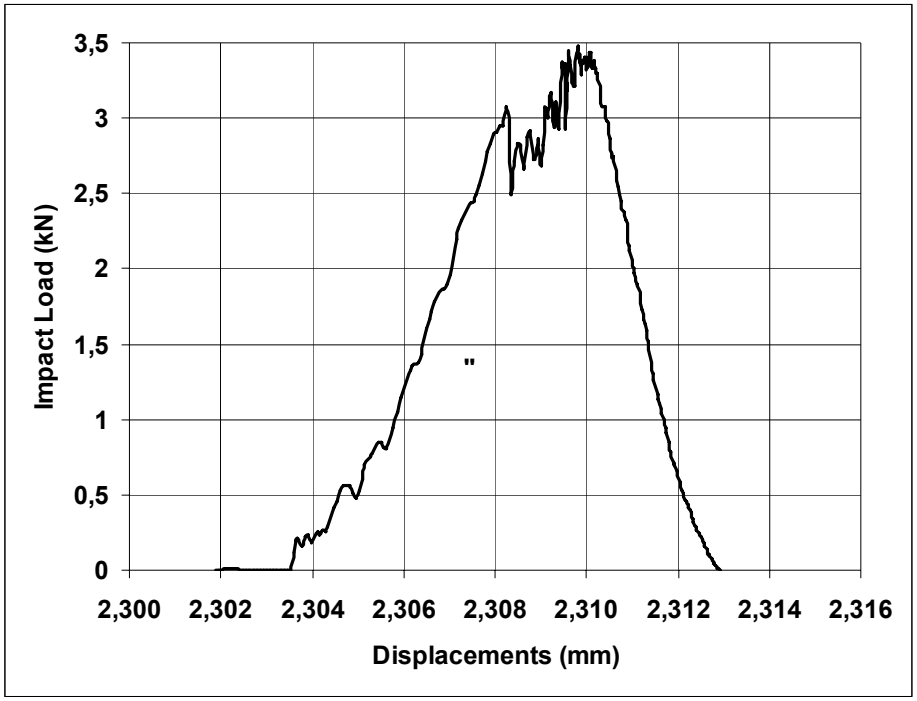

Figure 4.14 Displacement versus Load Diagram for Specimen C1

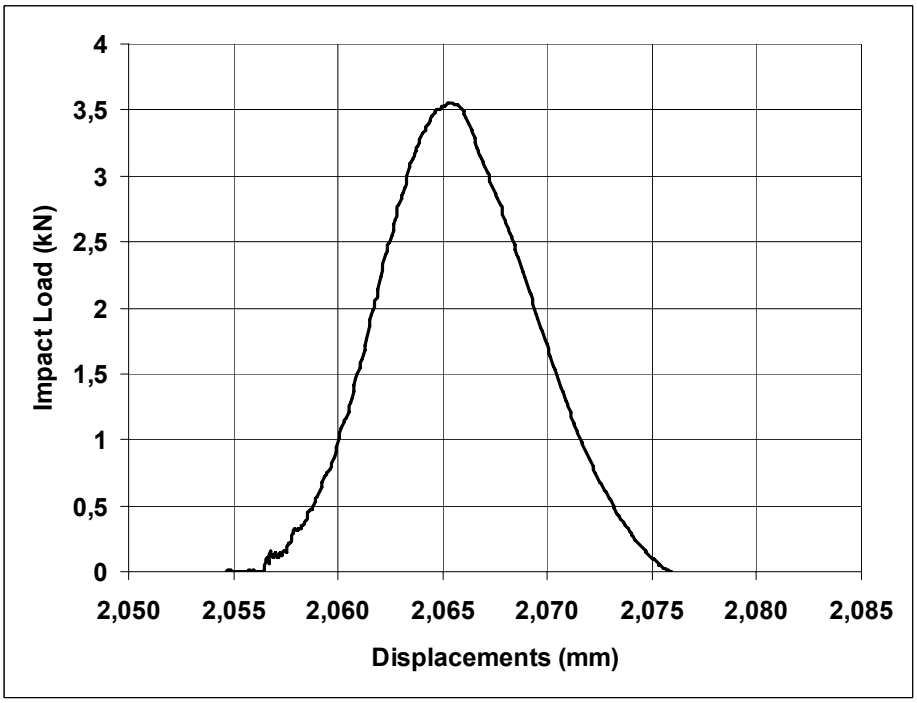

Figure 4.15 Displacement versus Load Diagram for Specimen A2

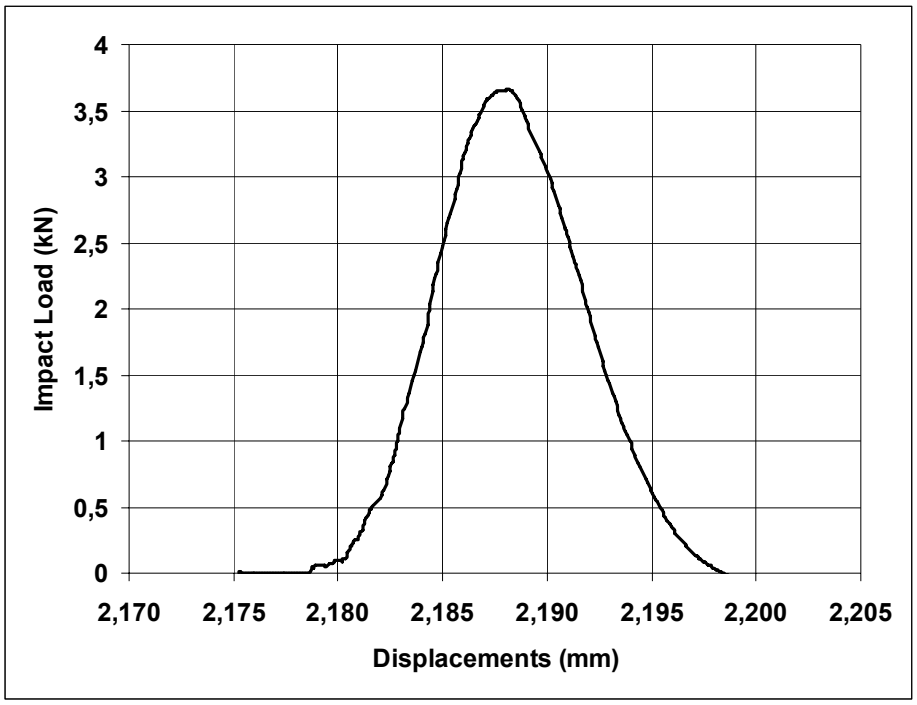

Figure 4.16 Displacement versus Load Diagram for Specimen H2

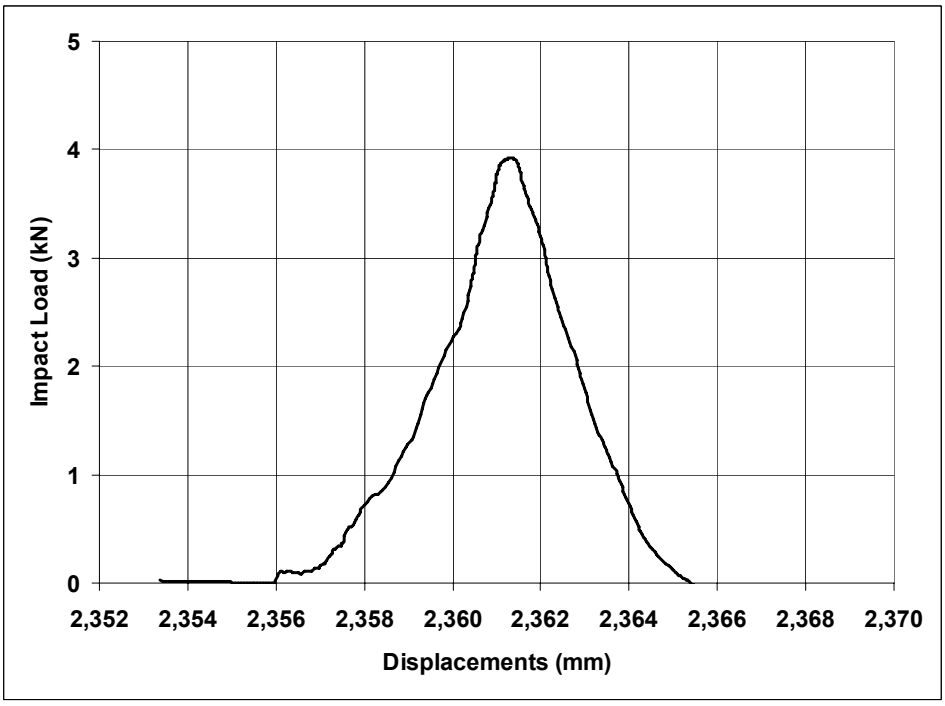

Figure 4.17 Displacement versus Load Diagram for Specimen H1

The impact energy of the specimens is calculated by using the area under the displacement versus impact load graphs. The results are shown in Figure 4.18. The aramid reinforced specimens A1, A2 and H2 show better impact energy behavior than the carbon reinforced specimen C2 and hybrid specimen H1. Furthermore, when the hybrid specimens are compared with each other, H2 has better damage behavior than H1. Although H2 is thinner than H1, because there are more aramid layers and fewer carbon layers the impact damage behavior is better. The specific impact energy of the specimens is also calculated to compare the weight effect on the impact energies which are shown as a bar graph in Figure 4.19. From this chart, A1 has the highest specific impact energy, because it is the thinnest specimen and its impact energy is also high when compared with the other specimens.

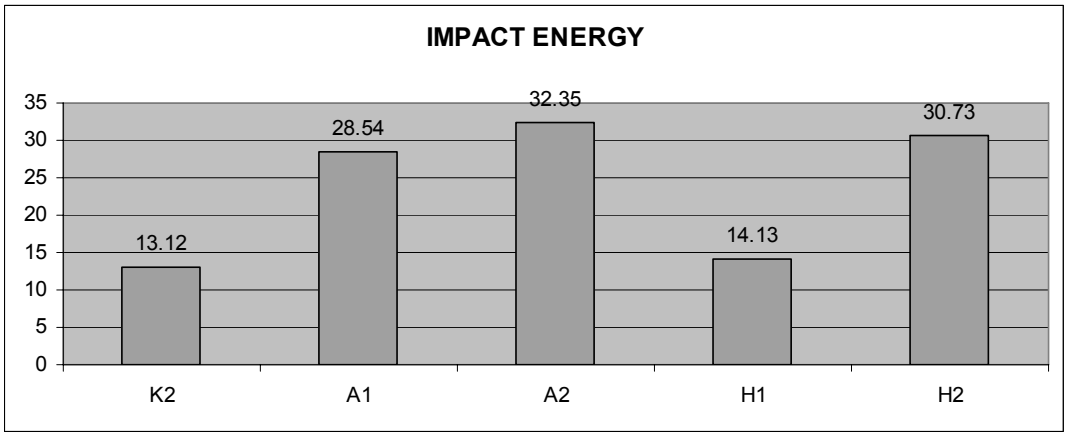

Figure 4.18 Impact Energy of Tested Specimens

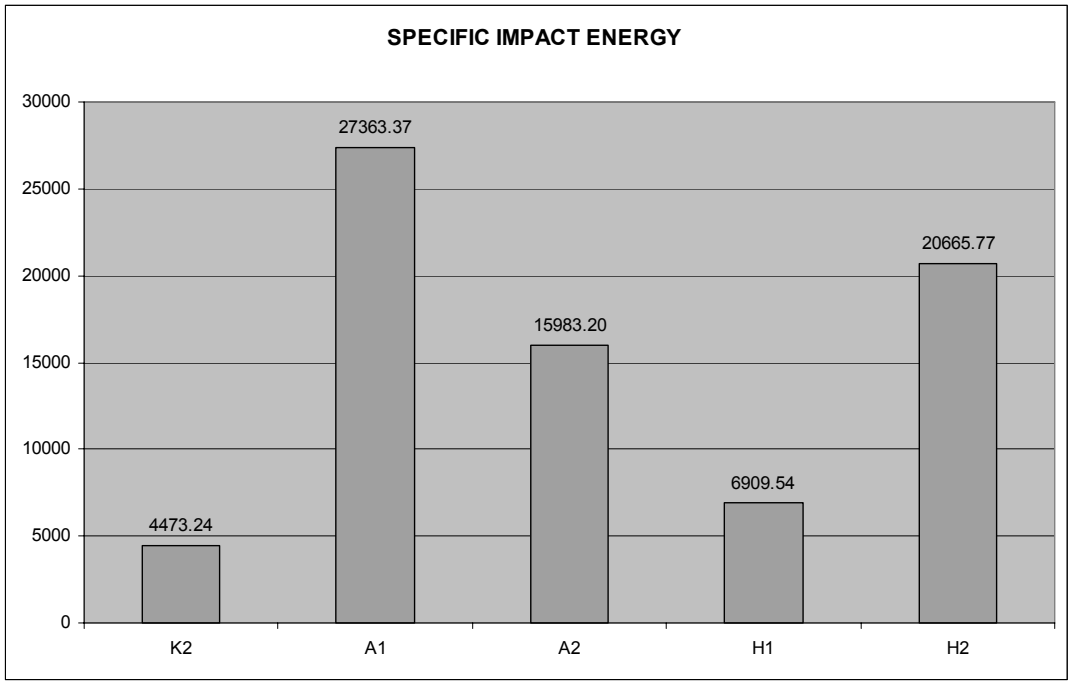

Figure 4.19 Specific Impact Energy of Tested Specimens

CHAPTER 5

THE HELMET SHELL DESIGN

5.1 Introduction

This chapter describes the design of the 3D helmet shell according to anthropometric data of members of the Turkish Army together with the subparts of the helmet system which have an impact on the shape and weight. The parameters for anthropometry came from the specified head measurements given by Kayıs et. al [31]. The PRO ENGINEER CAD program was used to create the 3D design of the helmet and give the anthropometric measurements to the headform model.

5.2 Helmet Shell 3D Design

The 3D helmet shell design was created according to ergonomic and geometric anthropometric data. Donelson and Gordon et al.[30] carried out an anthropometric survey on U.S Army Pilots and defined certain parameters for the measurement of head which are shown ,together with the descriptions, in Table 5.1. The diagrams of the parameters can be seen in Figures 5.1 to 5.5.

Table 5.1 Parameters of the Anthropometric measurements [30]

Measurement Parameter	**Measurement Definition (Donelson and Gordon, 1991)**
Head breadth	The maximum horizontal breadth above the attachment of the ears, measured with a spreading caliper.
Head circumference	The maximum circumference of the head above the attachment of the ears to the head, measured with a tape passing just above the ridges of the eyebrows and around the back of the head.
Head Length	The distance from the glabella landmark between the two brow ridges to the most posterior point on the back of the head, measured with a spreading caliper.
Interpupillary breadth	The distance between the two pupils, measured with a pupillometer.
Bitragion coronal arc	The surface distance between the right and left tragion landmarks across the top of the head, measured with a tape. The head is in the Frankfort plane.

.

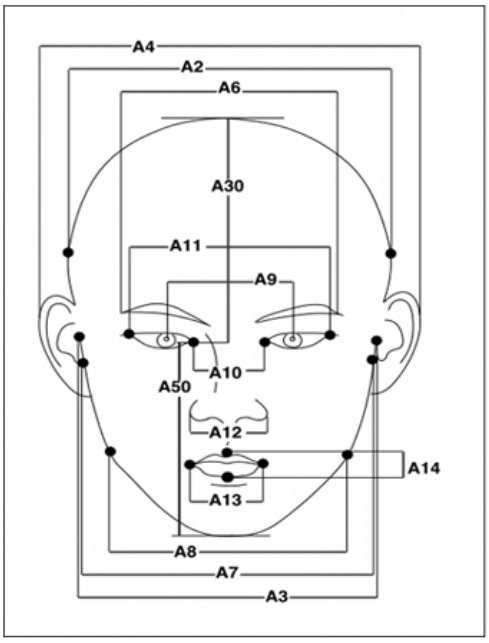

Figure 5.1 Face (Head) Breadth (A3)

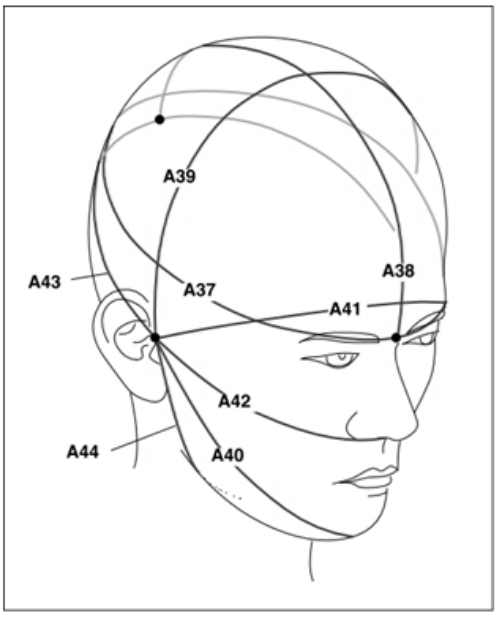

Figure 5.2 Head Circumference (A37)

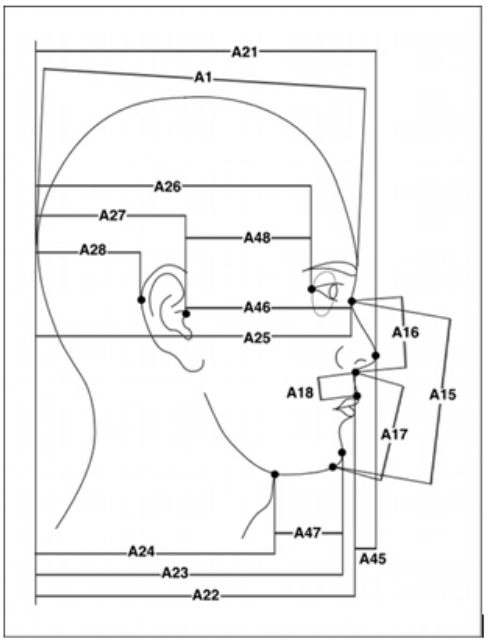

Figure 5.3 Head Length (A1)

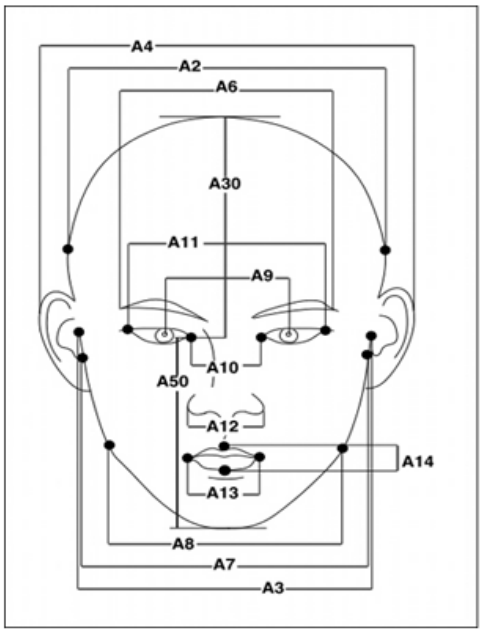

Figure 5.4 Interpupillary Breadth (A9)

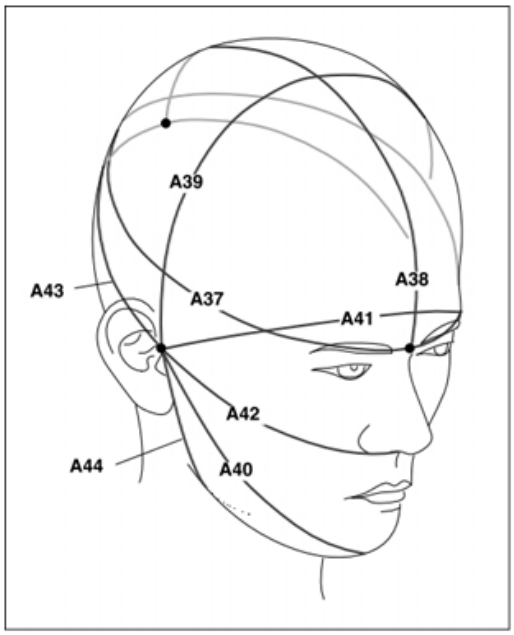

Figure 5.5 Bitragon Coronal Arc (A39)

After the composite material structural design stage, the 3D model of the helmet was created in the CAD program (PRO ENGINEER). Figures 5.6 to 5.8 show the helmet that was designed for this study using the parameters determined by Donelson and Gordon et. al [30] and the results of the survey by Kayış et. al [31] of the measurements of the heads of 5,109 men aged from 18 to 26 in the Turkish Army . The range and classification of the data used in the current study is shown in Table 5.2. The subparts of the helmet system; visor, liner, earcups and retention system were shown in Chapter 1 and can be seen on CAD model in Figure 5.6. The geometric size of the visor was used for the front side and the geometry of the retention system was used to create the inside shape of the helmet and the area covered by the earcups coverage.

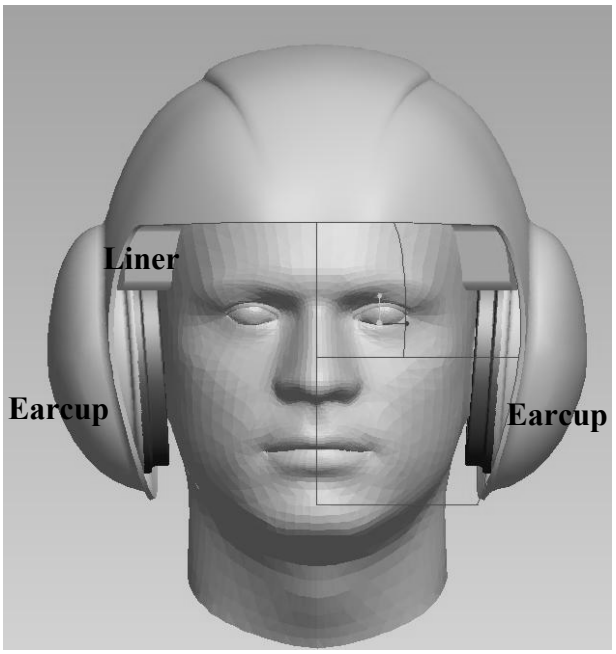

Figure 5.6 Front View of the Helmet Shell

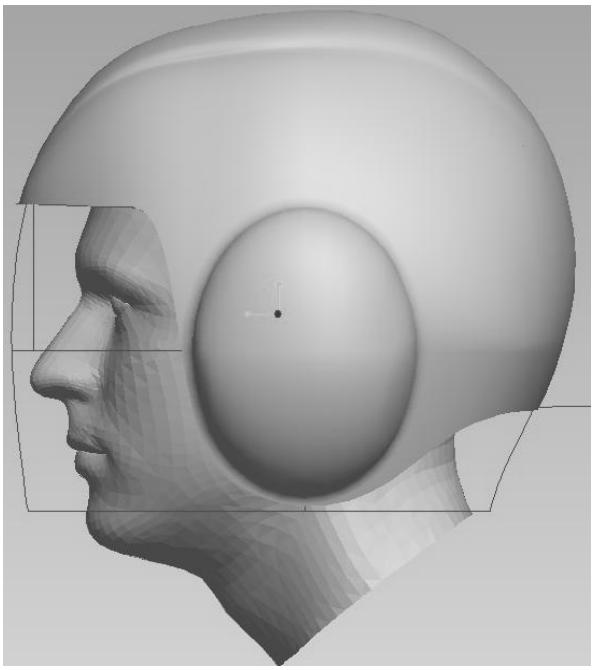

Figure 5.7 Side View of the Helmet Shell

Figure 5.8 General View of the Helmet Shell

Table 5.2 Geometric Design Data for Helmet Designed in the Current Study [31]

Variables	**5**	**50**	**75**	**90**	**95**
Weight (kg)	51.2	63.3	68.2	72.7	75.3
Face Breadth(cm)	12.4	13.8	14.3	14.6	15.8
Head Length(cm)	17.1	18.7	19.6	20	20.4
Distance between the eyes(cm)	5.4	6.1	6.5	6.7	6.9

After the completion of structural design, the experiment results of the composite specimens were evaluated for conformity to the light weight criteria and impact resistance. It was found that the material properties of the composite specimen H2 were suitable for the use of this material for the helmet shell. Combining the composite material selection and 3D shell design manufactured helmet is tested at Barış Elektrik Industry A.Ş. The details of the test rig and the results are presented in Chapter 6.

CHAPTER 6

IMPACT TEST SETUP AND THE EXPERIMENTAL RESULTS FOR THE HELMET SHELL

6.1 Introduction

In this part of the thesis, the impact tests of the designed 3D helmet shell are presented along with the experimental setup for helmet. The tested helmet was manufactured from the composite material according to the test results of the previous square plate experiments presented in Chapter 4. The impact tests were carried in Barış Elektrik company. According to the requirements of ANSI Z90.1 1992[32]. The test rig was constructed Barış Elektrik with contributions from Aselsan Inc. The aim of the impact tests was to measure the accelerations for all sides of the helmet shell as defined in the ANSI standard. Unlike the square specimen tests the data collection and subsequent calculations were not complicated since only one acceleration measurement was required and the result was evaluated as pass or fail for the helmet. In this chapter, detailed information of the test setup and the general statements of the results are presented.

6.2 Impact Points and Impact Description of the Helmet for the Impact Tests

The impact points and the steel anvils used during the impact tests are defined in ANSI Z90.1 1992[32]. In this standard, the application areas for the impact onto the

helmet shell are defined as 'the upper part of the test line for the four different areas of impact points(Figure 6.1). Therefore, protection is to be provided for the area shown in Figure 6.2.

Furthermore, the risk of impact at the sides of the earcup sides also needs to be taken into account, unfortunately, this standard could not confront the test procedure of impact points on the helmet shell for the earcup regions. Thus, the reference points for all vital impact areas and their acceleration levels as shown in Table 6.1 were taken from USAARL 96-04 report [39].

The impact description of the test procedure was also defined before starting the impact tests. The tests were carried out on all parts of the helmet including the sub parts (retention system, earcups and liner). A total 7 different impact areas on the helmet shell were tested according to both the ANSI Z90.1 1992[32] standard and the USAARL 96-04 report with (Figure 6.3). Each helmet were impacted at least two of them on flat anvil and at least two of them again on semi spherical anvil. Furthermore, each helmet was impacted also 6.3 mm edge steel anvil once. The helmet was dropped on to the anvils at a velocity of 6 m/s. The helmet module with its subparts was dropped from 220 cm. to provide this velocity level.

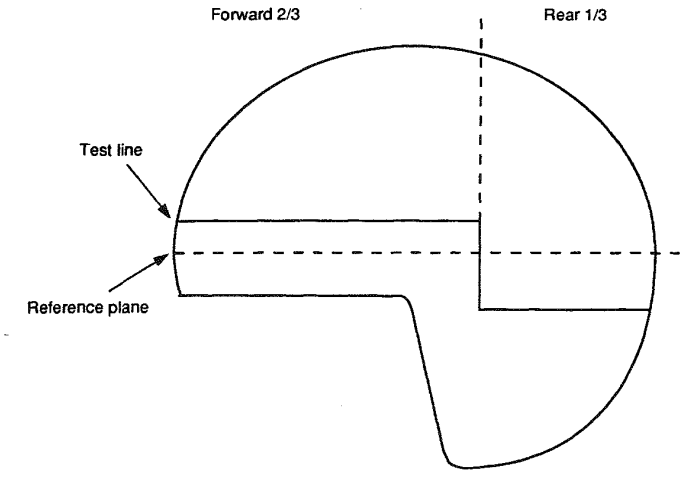

Figure 6.1 Test Line Location [32]

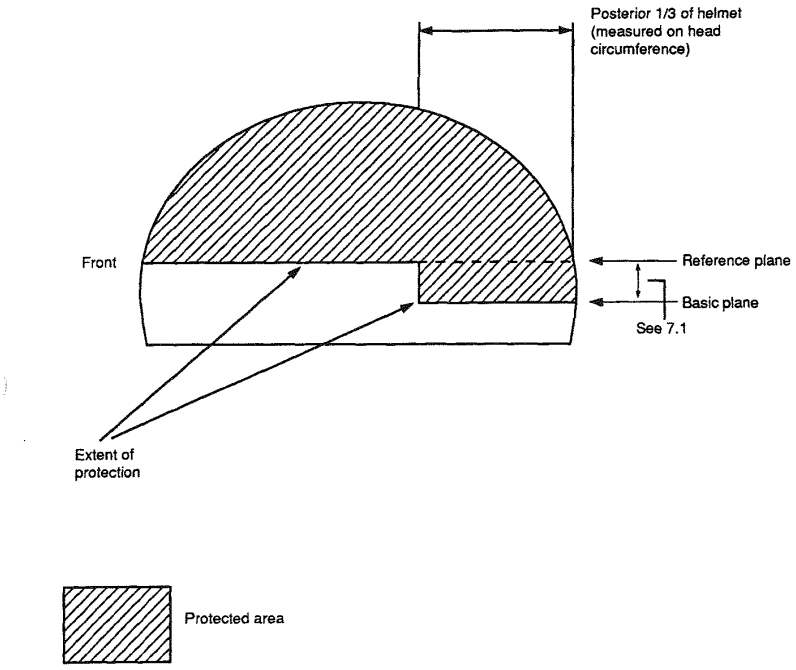

Figure 6.2 Protection Areas of the Helmet Shell [32]

Table 6.1 Defined Test Points on the Helmet Shell and Anvils Used

Impact Points	**Min. Acceleration (g)**	**Anvil Type**
Left Earcup	300	Semi Spherical
Right Earcup	300	Semi Spherical
Front Side	300	Semi Spherical
Left Side	300	Flat
Right Side	300	Flat
Upper Side	300	Flat
Back Side	300	6,3 mm

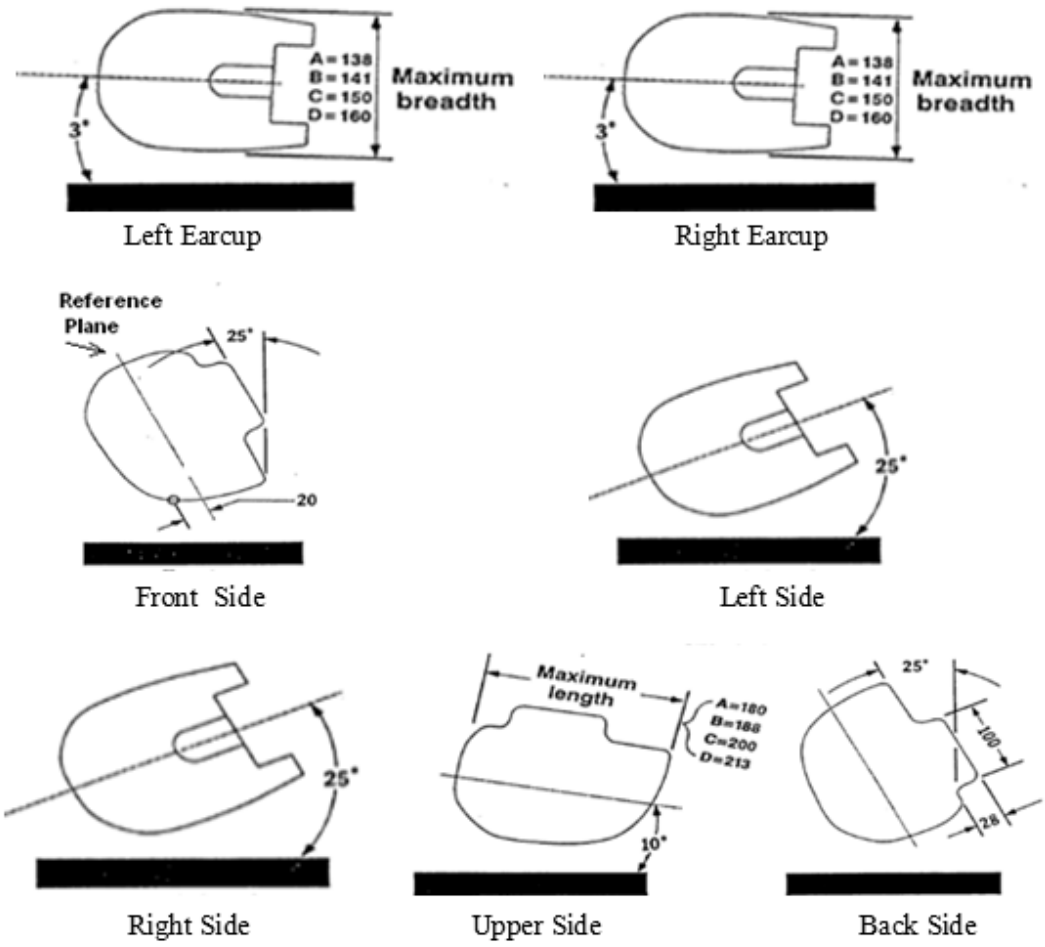

Figure 6.3 Impact Test Points [39]

6.3 Experimental Setup and Devices of the Impact Test

In this section the comparison of the specimen test rigs and helmet test rigs are reported. Because of the impacted items are different there are some differences between two setup. Furthermore, the setup's subparts are also introduced in a detailed way.

6.3.1 Experimental Setup

The test rig (Figure 6.5) for the helmet shell was located in Barış Elektrik Industries. As reported in Chapter 3 this setup was similar to the previous redesigned experimental setup, the main difference was the dropping item. The drop weight was a hammer in the previous redesigned setup, however in the Baris Elektrik setup's the helmet was dropped on to the anvils. The tested specimens' setup had no catching mechanism to prevent the rebound.

The subparts of the set up for the helmet impact tests were monorail tower, planetary mechanism, headform with its connection arm, catching mechanism to prevent the rebound, accelerometers and the velocity sensors located at the side of the tower.

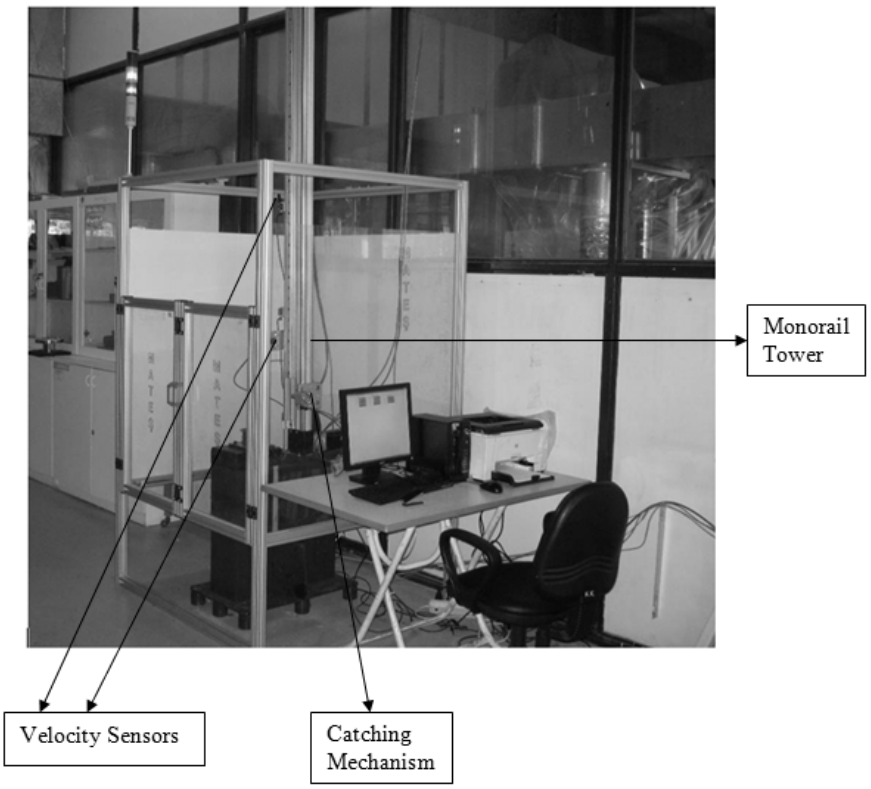

Figure 6.4 General View of Helmet System's Experimental Setup in Barış Elektrik Industries Facilities

6.3.2 Headform

The chosen headform was made from magnesium alloy. The dimensions of this headform should meet the standards stated in DOT FMVSSS 218 or ISO/DIS 6220 and they are defined in ANSI Z90.1 1992[32]. The headforms used for the impact tests were cast according to the DOT standard. After the casting process, the human headform sizes were applied to the casted headform by a CNC operation. For the helmet impact drop test. The headform should be;

- mounted to the test setup by a connection arm with a total weight (headform and the mounting arm) of 5 kg + 0.2/-0.0 kg. This connection arm was made of aluminum and of spherical shape. The sphere is hollow and this is where the accelerometer was located (Figure 6.5). The other side of the connection arm was placed on the planetary mechanism of the experimental setup and can be moved on the monorail system.
- mounted by the intersection of the headform reference plane and the helmet reference plane(shown in Figure 6.1)
- with the helmet in a stable position during the free fall of the helmet.
-

Figure 6.5 Headform and Connection Arm

6.3.3 Accelerometer

The used piezoelectric accelerometer had the ability to measure along three axes and the measuring capacity was up to 2000g ± 400g. The velocity was measured by the sensors during the impact test. Two sensors were placed along the side of the monorail 50 cm apart as shown in Figure 6.4. When the planetary mechanism was moving past the sensors the time was measured, and from this data the distance velocity can be calculated. Also, the velocity prior to the impact was calculated by energy formulations.

6.3.4 Anvils

Helmet was dropped onto three different shaped steel anvils which were mounted on the setup as required. Their properties are defined in ANSI Z90.1 1992 [32]. The flat anvil had a diameter of 127 mm; the hemispherical anvil had a radius of 48 mm and the 6.3 mm anvil had a 6.3 mm width x 18 cm length x 10 cm height protrusion (Figure 6.6).

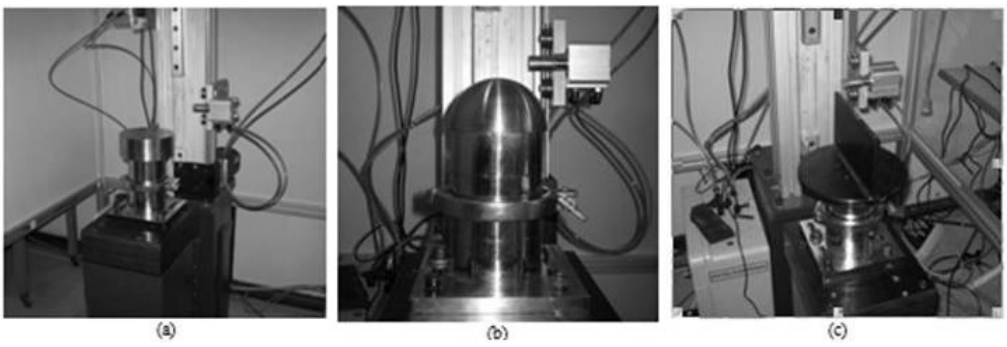

Figure 6.6 Steel Anvils (a) Flat Anvil (b) Semi Spherical Anvil (c) 6.3 mm Anvil

6.4 Results and Discussions of the Impacted Helmet

The composite specimen H2 was used to manufacture the helmet. The impact tests were undertaken on the manufactured helmet for each of the defined impact points.

To show how the test was performed the three photographs in Figure 6.7 show the successive steps until the impact test was completed. After the specified tests were carried out, it was seen that the measured acceleration levels were below 300 g for all 7 impact points defined on the helmet which is complies with the ANSI standard. Thus, it is concluded that the hybrid H2 helmet which passed the tests mentioned above can be considered to be a safe helicopter helmet ensuring the pilot survivability when the impact energies to the helmet are below 300 g.

Figure 6.7 General View of the Impact Test Rig for the Helmet Shell

CHAPTER 7

CONCLUSION AND SUGGESTIONS FOR FUTURE WORK

This thesis investigated the effects of different material combinations on the design of a helicopter helmet shell with respect to impact performance and compliance with the criteria of being sufficiently lightweight. To achieve the final product; a literature survey, material and setup selection and impact experiments were performed.

From the literature, drop weight impact tests and the used composite specimens under low velocity impacts were reviewed and the composite material type and appropriate setup were chosen. Aramid, carbon and hybrid specimens (aramid and carbon reinforced) were chosen for impact absorption testing. For the impact test setup, Gazi University Civil Engineering Laboratories' Drop Weight Impact Setup was used with some modifications, such as the addition of the specimen holder housing. The other parts of the experimental setup such as the accelerometers, load cells and optical photocells were selected and correctly adjusted. The accelerometers have been chosen according to the 300g maximum acceleration value required in the helmet test standard ANSI Z90.1 1992[32] . The load cell was chosen to read the maximum load value (4 tons) after the impact of a drop weight of 5.25 kg. The diffusive optical photocells were used to measure the time for the experiment as described in Chapter 3. In addition the hammer connected to the chrome rails (kestamid rollers) of the drop weight tower and the specimen holder housing comprised the mechanical parts of the setup.

To find the best material combination, composite test specimens were produced for testing under the impact drop weight. The stacking sequence of tested specimens were chosen as $[0/90]_i$ according to previous studies found in the literature and the advice of the industrial manufacturer. From the results of impact tests, Time vs. Acceleration, Time vs. Velocity, Time vs. Displacement, Time vs. Impact Load and Displacement vs. Impact Load graphs were created. This was made possible by the utilization of a data acquisition device for data transfer and the computer program DIADEM for processing.

As can be seen from the results of the experiments, specimens that are manufactured from different materials behaved differently under impact. The C1 and C2 specimens manufactured from carbon fibers reached very large accelerations values, when the drop hammer was released from a height of 30 cm. These samples showed small displacements and dissipated small amount of energy.

From the same drop height 30 cm the A1 and A2 specimens manufactured from aramid showed more displacement when compared to carbon fiber specimen. In addition, the acceleration values are particularly lower than the carbon ones. The aramid specimens showed a dominantly ductile behavior and there were visible displacements. The drop weight made greater rebounds on the aramid samples. Although, the base drop height was kept constant at 30 cm. However, for the aramid samples a constant weight was dropped from 50 and 70 cm to see capacity of impact at higher drop heights were used on some of the other tested specimens This could be further investigated in future studies. . The measured displacement and maximum accelerations increased significantly with the increasing drop height as summarized in Table 4.3. The numbers of rebounds decreased with the increasing internal damages. The aramid specimens dissipated more energy than the C2 carbon specimen.

The final series tests were carried out on the hybrid specimens consisting of aramid and carbon fiber layers. The behavior of the H1 and H2 hybrid specimens were a mix of the behaviors of the individual samples of aramid and carbon. The hybrid

specimens displayed respectively more ductile and brittle behavior than the carbon and aramid specimens. The accelerations from hybrid specimens, when the drop weight (hammer) was dropped from 30 cm, were smaller than those of the carbon specimens. The constant weight hammer was dropped from a height of 50 cm to reach the maximum damage capacity of the hybrid specimens. The displacement and maximum accelerations increased with the increasing drop height. The energy dissipation capacities of the hybrid specimens were greater than for the carbon specimens and close to measurements obtained from the aramid specimens.

In conclusion the test results of all six specimens, hybrid composite specimens H1, H2 and Aramid composite specimens A1, A2 gave better performances of acceleration compared to the carbon reinforced samples. Moreover, when the impact energy of specimens calculated from the area under the Displacement vs. Impact Load graphs the H2, A1 and A2 specimens gave optimum performance in terms of impact strength. In particular the aramid A2 specimen was able to carry large impact loads and dissipate a large amount of energy. The time vs. velocity, displacement and force graphical results as shown in Chapter 4 show to according to the impact energy and acceleration results H2 gave the optimum performance. Thus, this composite material was selected to manufacture the model helicopter helmet shell.

In the final stage, manufactured helmet shell which was manufactured from the same composite structure as the H2 specimen and designed in a 3D CAD program according to the antropometric data, was tested according to the ANSI standard on a helmet impact test rig. The helmet fulfilled the 300 g acceleration criteria on the designated seven impact points.

This study has shown how an advanced helicopter helmet was designed from beginning to the production of a sample helmet. How to design a helicopter helmet including the standards and requirements, the necessary test setup with its devices and the appropriate composite types has been presented sequentially stage by stage. The end product is a new lightweight composite structure for a helicopter helmet

shell, which is able to withstand a low velocity impact.

The suggestions for future work include, using different stacking sequences and composite materials combinations further, higher drop heights can be used to test the durability and safety of the helmet. Being lightweight is a crucial requirement for a helmet system because pilot's head can only bear a limited weight. Therefore, designers should extend the search for research new composite material combinations to create lighter and more impact resistant helicopter pilot helmets.

REFERENCES

[1] Sayer, M., Bektaş, N.B., Çallioğlu, H. (2010). Impact Behavior of Hybrid Composite Plates. *Journal of Applied Polymer Science,* 118, 580-587.

[2] Her, S.C., Liang, Y.C. (2004). The finite element analysis of composite laminates and shell structures subjected to low velocity impact. *Composite Structures,* 66, 277-285.

[3] Sayer, M., Bektaş, N.B., Sayman, O. (2010). An experimental investigation on the impact behavior of hybrid composite plates. *Composite Structures,* 92, 1256-1262.

[4] Kostopoulos, V., Markopoulos, Y.P., Giannopoulos, G., Vlachos, D.E. (2002). Finite element analysis of impact damage response of composite motorcycle safety helmets. *Composites: Part B,* 33, 99-107.

[5] Padaki, N.V., Alagirusamy, R., Deopura, B.L. (2008). Low velocity impact behavior of textile reinforced composites. *Indian Journal of Fibre and Textile Research,* 33, 189-202.

[6] Naik, N.K., Sekher, Y. C., Meduri, S. (2000). Damage in woven-fabric composites subjected to low-velocity impact. *Composites Science and Technology,* 60, 731-744.

[7] Belingardi, G., Vadori, R. (2002). Low velocity impact tests of laminate glass-fiber-epoxy matrix composite material plates. *International Journal of Impact Engineering,* 27, 213-229.

[8] Belingardi, G., Vadori, R. (2003). Influence of the laminate thickness in low velocity impact behavior of composite material plate. *Composite Structures,* 61, 27-38.

[9] Choi, H.Y, Chang, F.K. (1992). A Model for Predicting Damage in Graphite/Epoxy Laminated Composites Resulting from Low-Velocity Point Impact. *Journal of Composite Materials,* 26, 2134-2169

[10] Chang, F.K, Chang, K.Y. (1987). A Progressive Damage Model for Laminated Composites Containing Stress Concentrations. *Journal of Composite Materials,* 21, 834-855.

[11] Iannucci, L. (2006). Progressive failure modelling of woven carbon composite under impact. *International Journal of Impact Engineering,* 32, 1013-1043.

[12] Hou, J.P., Petrinic, N., Ruiz, C., Hallett, S.R. (2000). Prediction of impact damage in composite plates. *Composites Science and Technology,* 60, 273-281.

[13] Hosseinzadeh, R., Shokrieh, M.M., Lessard, L. (2006). Damage behavior of fiber reinforced composite plates subjected to drop weight impacts. *Composites Science and Technology,* 66, 61-68.

[14] Sevkat, E., Liaw, B., Delale, F., Raju, B.B. (2006). Damage behavior of fiber reinforced composite plates subjected to drop weight impacts. *Composites Part A,* 40, 1090-1110.

[15] Aslan, Z., Karakuzu, R., Okutan, B. (2003). The response of laminated composite plates under low-velocity impact loading. *Composite Structures,* 59, 119-127

[16] Hitchen, S.A., Kemp, R.M.J. (1995). The effect of stacking sequence on impact damage in carbon fibre/epoxy composite. *Composites*, 26, 207-214.

[17] Richardson, M.O.W., Wisheart, M.J. (1996). Review of low-velocity impact properties of composite materials. *Composites Part A*, 27, 1123-1131.

[18] Strait, L.H., Karasek, M.L., Amateu, M.F. (1992). Effects of Stacking Sequence on the Impact Resistance of Carbon Fiber Reinforced Thermoplastic Toughened Epoxy Laminates. *Journal of Composite Materials*, 26, 1725-1740.

[19] Cantwell, W.J., Morton, J. (1991). The impact resistance of composite materials – a review. *Composites*, 22, 347-362

[20] Cernicchi, A., Galvanetto, U., Iannucci, L. (2007). Virtual Modelling of Motorcycles Safety Helmets: Practical Problems. *6th European LS-DYNA Users' Conference*, 5.223-5.232.

[21] HISL® Alpha Eagle 900 techical data sheet, ASELSAN Inc. Library

[22] Type of Loadcells Information, http://www.e3tam.com/temsilcilikler/pcb/kuvvet.htm, last visited on 20 April 2011

[23] Type of Photocells Information, http://www.infotek.com.tr/banner.htm

[24] Abrate S. (1994). Impact on laminated composites: Recent advances. Appl. Mech Rev, vol. 47 no. 11, 517-544

[25] Dahsin L., Basavaraju B.R, Xinglai D. (2000). Impact perforation resistance of laminated and assembled composite plates. *International Journal of Impact Engineering*, 24, 733-746

[26] Hampson P.R, Moatamedi M. (2007). A review of composite structures subjected to dynamic loading. *International Journal of Crashworthiness*, 12: 4, 411-428.

[27] Peters S. T., *Handbook of Composites*, 2nd edition, Chapman andHall, California, 1998.

[28] Definition of hybrid composite, http://composite.about.com/library/glossary/h/bldef-h2698.htm, last visited on 15 March 2011

[29] MacEntire B. J., U.S Army Aircrew Helmets:Heaad injury mitigation technology, U.S. Army Aeromedical Research Laboratory USAARL, Report No: 98-12, 1998.

[30] Donelson, S.M., and Gordon, C.C. (1991). Anthropometric survey of U.S. Army personnel:Pilot summary statistics. Natick, MA: U.S. Army Natick Research, Development, Engineering Center. Technical Report TR-91040.

[31] Kayış (1991). The anthropometry of Turkish Army men. Aselsan Library.

[32] ANSI Z90.1 1992, American National Standard Specification for Protective Headgear for Vehicular Users, Aselsan Libraray.

[33] McEntire B.J., Whitley P. (2005). Blunt Impact Performance Characteristics of the Advanced Combat Helmet and The Paratrooper and Infantry Personnel Armor System for Ground Troops Helmets. USAARL Technical Report No. 2005-12.

[34] PCB Piezotronics Accelerometer Spec Sheet, http://pcb.com/spec_sheet.asp?model=353B02, last visited on 30 March 2011

[35] PCB Piezotronics Load Sensor Spec Sheet, http://www.pcb.com/spec_sheet.asp?model=202Banditem_id=2298, last visited on 21 April 2011

[36] Gentex® HGU56 Helicopter Helmet technical data sheet, ASELSAN Library.

[37] Gentex® SPH 4B Helicopter Helmet technical data sheet, ASELSAN Library.

[38] Kantar, E., "CFRP ile Güçlendirilmiş Beton Kirişlerin Çarpma Davranışının Deneysel Olarak İncelenmesi", Gazi Üniversitesi, Fen Bilimleri Enstitüsü, Ankara, 2009.

[39] U.S. Army Aeromedical Research Laboratory USAARL, Report No: 96-04

APPENDIX A

TECHNICAL SPECIFICATIONS OF THE PIEZOELECTRIC ACCELEROMETER

Table A.1 Technical specifications of accelerometer model 353B02 [34]

Performance	Value
Sensitivity(± 5 %)	2.04 mV/(m/s²)
Measurement Range	± 2453 m/s²
Frequency Range(± 5 %)	1 to 7000 Hz
Frequency Range(± 10 %)	0.7 to 10,000 Hz
Frequency Range(± 3 dB)	0.35 to 18,000 Hz
Resonant Frequency	≥ 38 kHz
Broadband Resolution(1 to 10,000 Hz)	0.05 m/s² rms
Non-Linearity	≤ 1 %
Transverse Sensitivity	≤ 5 %
Overload Limit(Shock)	± 98,100 m/s²
Temperature Range(Operating)	-54 to +121 °C
Excitation Voltage	18 to 30 VDC
Constant Current Excitation	2 to 20 mA
Output Impedance	≤ 100 ohm
Output Bias Voltage	8 to 12 VDC
Discharge Time Constant	0.5 to 2.0 sec
Settling Time(within 10% of bias)	<5 sec
Sensing Element	Quartz
Electrical Connector	10-32 Coaxial Jack
Electrical Connection Position	Top
Weight	10 gm

APPENDIX B

TECHICAL SPECIFICATIONS OF LOAD SENSOR

Table B.1 Technical specifications of the ring quartz force sensor 202B ICP [35]

Performance	Value
Sensitivity(± 5 %)	112.4 mV/kN
Measurement Range	44.48 kN
Low Frequency Response (-5%)	0.0003 Hz
Upper Frequency Limit	60 kHz
Broadband Resolution(1 to 10,000 Hz)	0.890 N-rms
Non-Linearity	≤ 1 %
Temperature Range(Operating)	-54 to +121 °C
Excitation Voltage	20 to 30 VDC
Constant Current Excitation	2 to 20 mA
Output Impedance	≤100 ohms
Output Bias Voltage	8 to 14 VDC
Discharge Time Constant	≥ 2000 sec
Electrical Connector	10-32 Coaxial Jack
Electrical Connection Position	Side
Weight	19 gm

APPENDIX C

TECHNICAL SPECIFICATIONS OF DATA ACQUISITION DEVICE

Table C.1 Technical specifications of data acquisition device NI 9233-USB-9162 [38]

Performance	Value
Number of channels	4 analog input channels
Resolution	24 bits
Spurious-free dynamic range (SFDR)	102 dB
Minimum Data Ratio	2 kS/s
Maximum Data Ratio	50 kS/s
Frequency	12.8 MHz
Accuracy	± 100 ppm max.
Input Coupling	AC
Minimum AC Voltage	5 V
Maximum AC Voltage	5,8 V
Minimum IEPE Excitation Current	-54 to +121 °C
Input Voltage Interval	± 5 V
BUS Interface	USB 2.0 high speed

APPENDIX D

TECHNICAL DRAWINGS OF TOOLS DESIGNED FOR TEST SETUP

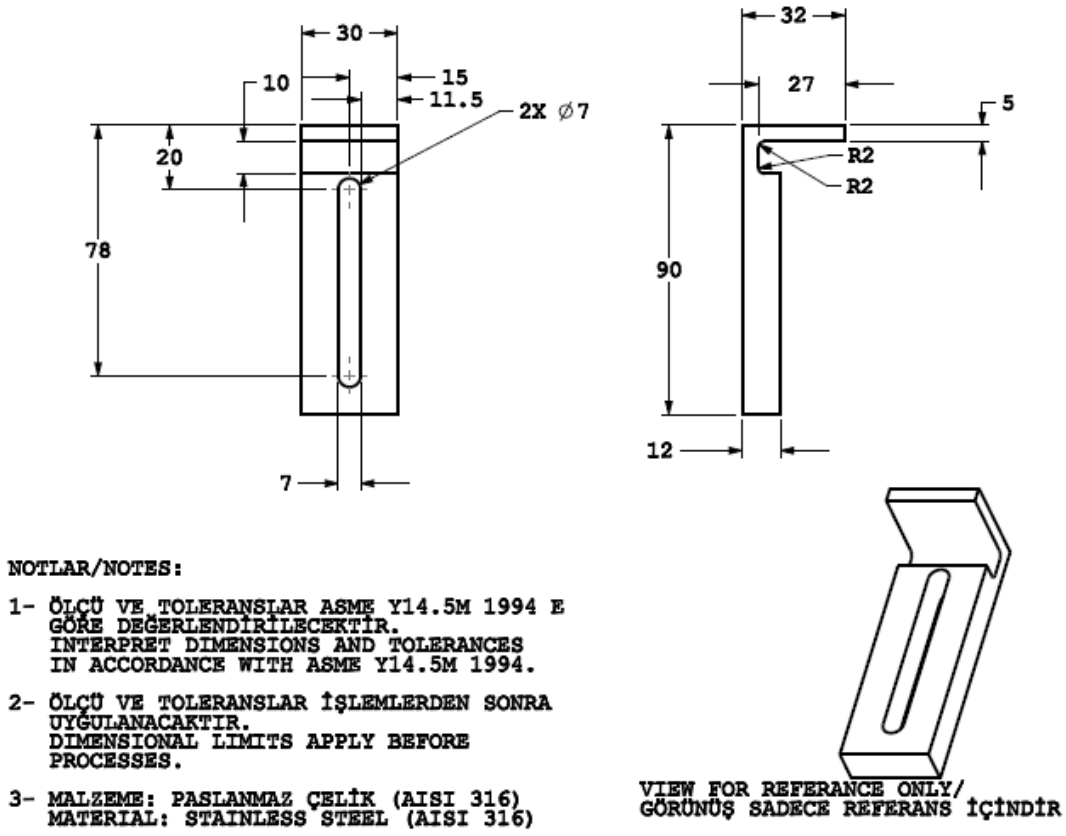

Figure D. 1 Technical Drawing of Support Clamps

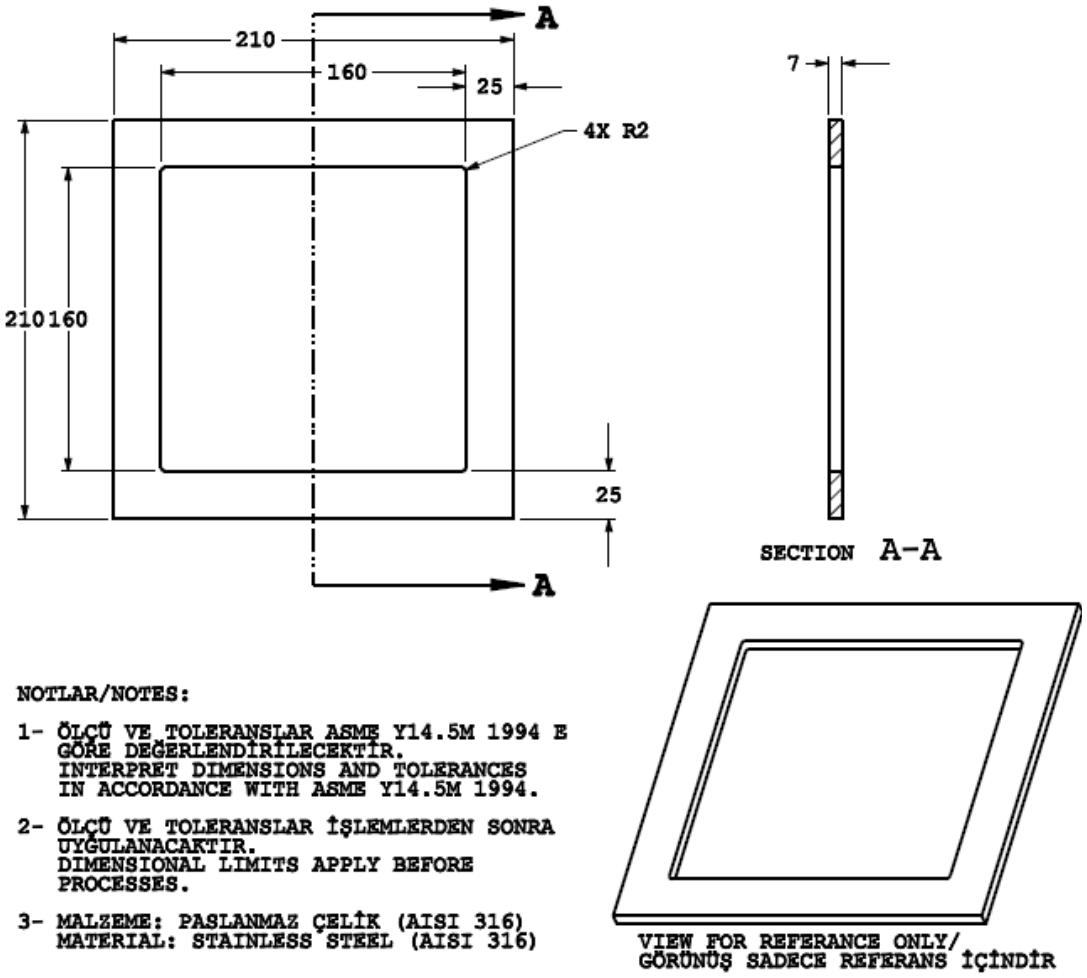

Figure D. 2 Technical Drawing of Support

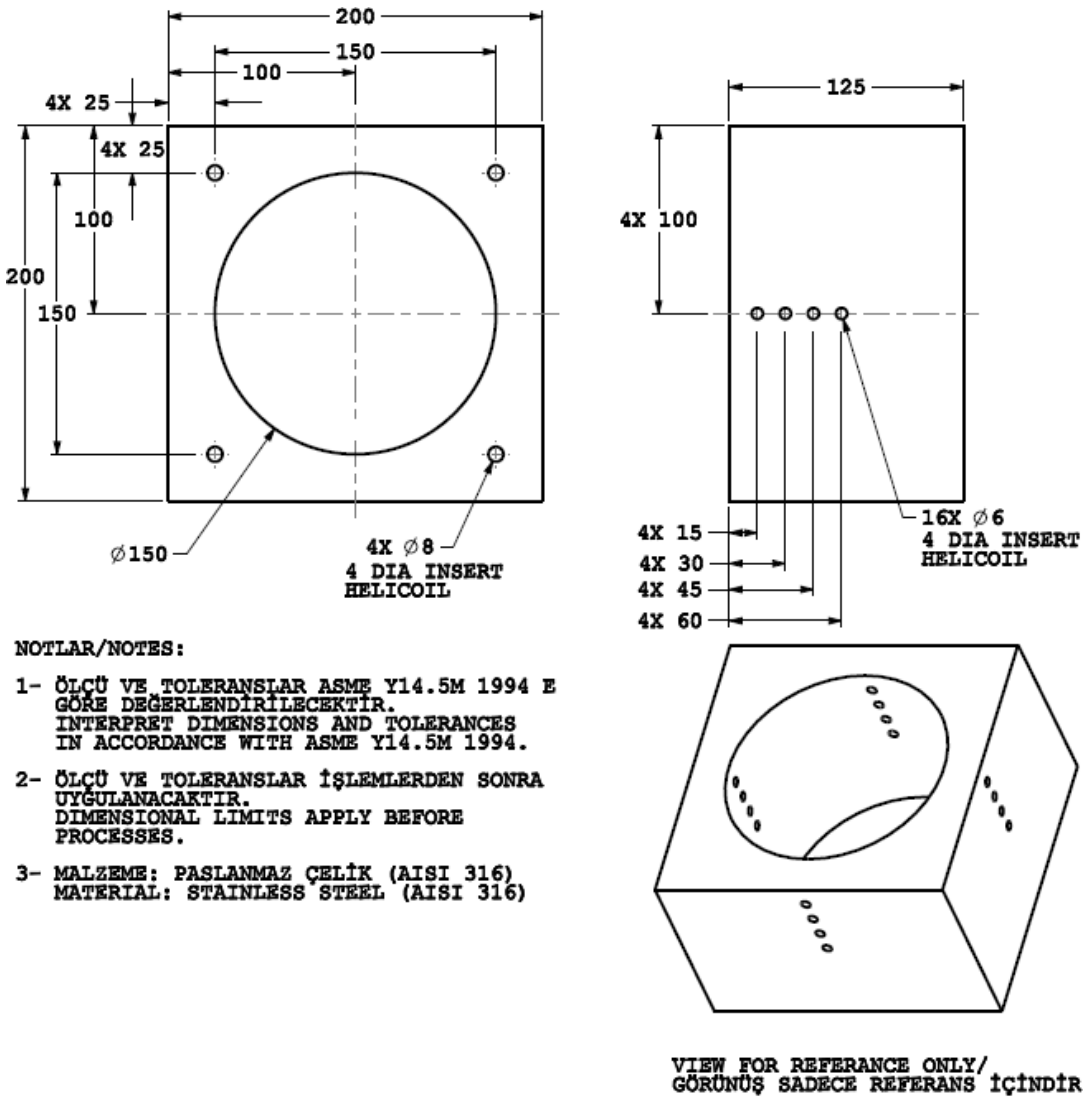

Figure D. 3 Technical Drawing of Upper Test Block

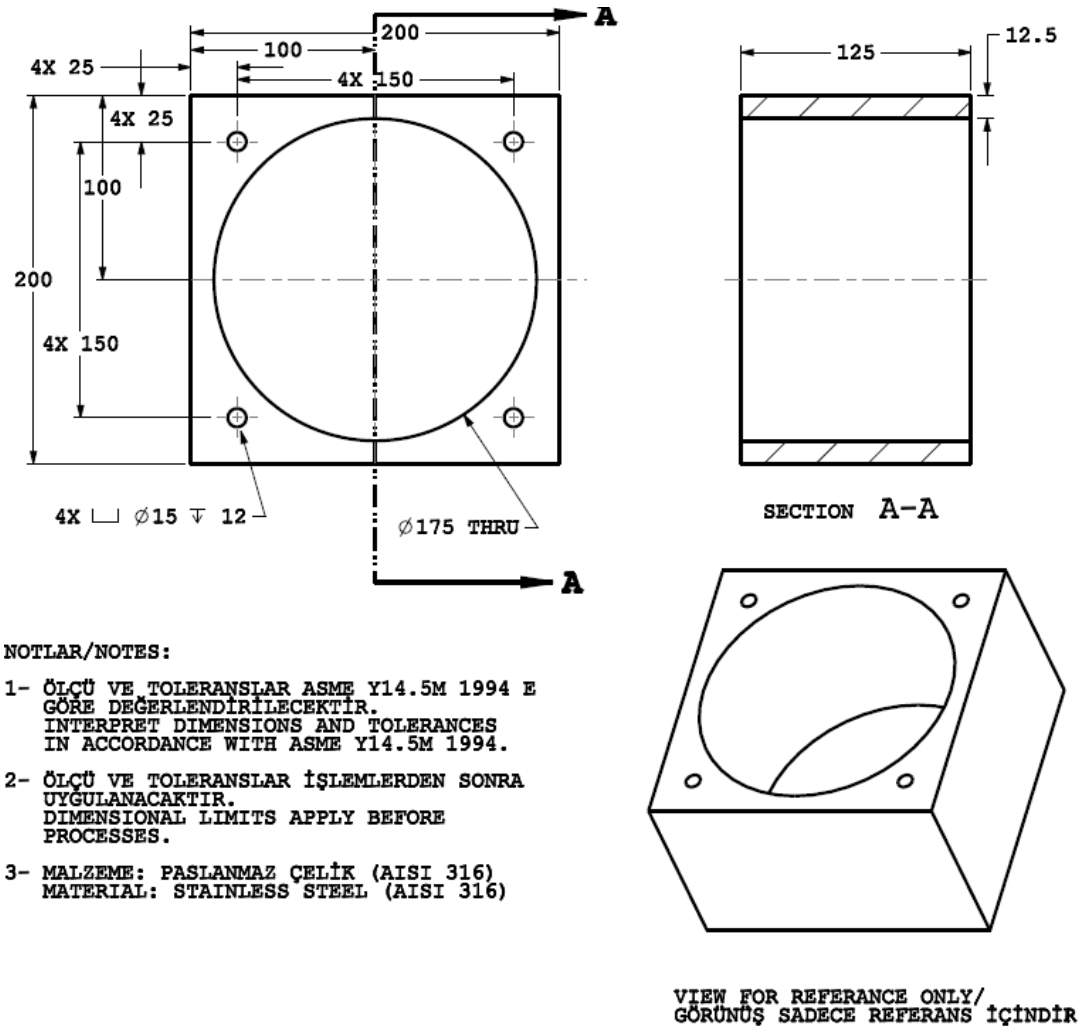

Figure D. 4 Technical Drawing of Lower Test Block